

Light Higgs and Vector-like Quarks without Prejudice

Svjetlana Fajfer,^{1,2,*} Admir Greljo,^{1,†} Jernej F. Kamenik,^{1,2,‡} and Ivana Mustac^{1,§}

¹*Jozef Stefan Institute, Jamova 39, 1000 Ljubljana, Slovenia*

²*Faculty of Mathematics and Physics, University of Ljubljana, Jadranska 19, 1000 Ljubljana, Slovenia*

(Dated: September 27, 2018)

Light vector-like quarks with non-renormalizable couplings to the Higgs are a common feature of models trying to address the electroweak (EW) hierarchy problem by treating the Higgs as a pseudo-goldstone boson of a global (approximate) symmetry. We systematically investigate the implications of the leading dimension five operators on Higgs phenomenology in presence of dynamical up- and down-type weak singlet as well as weak doublet vector-like quarks. After taking into account constraints from precision EW and flavour observables we show that contrary to the renormalizable models, significant modifications of Higgs properties are still possible and could shed light on the role of vector-like quarks in solutions to the EW hierarchy problem. We also briefly discuss implications of higher dimensional operators for direct vector-like quark searches at the LHC.

I. INTRODUCTION

The recent LHC discovery of a Higgs boson [1] seems to experimentally complete the standard model (SM) picture of fundamental interactions. Although the SM works extremely well phenomenologically, the electro-weak (EW) hierarchy problem, as exemplified by the extreme UV sensitivity of the Higgs potential, provides a strong theoretical motivation for contemplating beyond SM physics at the TeV scale.

On the other hand, direct searches for on-shell production of new degrees of freedom at the LHC together with ever more stringent constraints from measurements of flavor, EW and Higgs observables are starting to directly probe models addressing the naturalness problem of the SM. At present these experimental null-results are not yet conclusive, but viable new physics (NP) models' parameter space is becoming significantly reduced. In light of this, it has become crucial to focus on the minimal light particle content required to fulfil the naturalness conditions (see [2] for examples in supersymmetric theories).

Vector-like quarks are expected to be the lightest new degrees of freedom in models addressing the EW hierarchy problem by treating the light Higgs as a pseudo-goldstone boson of a global symmetry, broken explicitly by the SM gauging and Yukawa couplings [3, 4]. In such models, the dominant quadratic divergences in one-loop corrections to the Higgs boson mass coming from the top quark loop are canceled by contributions of dimension five operators of the form $H^\dagger H Q Q$, where H is the Higgs doublet and Q a vector-like quark weak multiplet. In general, parametrizing single- and double-Higgs interactions of an arbitrary number of quark flavors f in the mass eigenbasis

$$\mathcal{L}_h^{\text{eff}} = \left(-y_{ij} h + x_{ij} \frac{h^2}{2v} \right) \bar{f}_L^i f_R^j + \text{h.c.}, \quad (1)$$

where $v = (\sqrt{2}G_F)^{-1/2} \simeq 246$ GeV is the EW condensate, the condition for cancelation of one-loop quadratic divergences from such interactions can be put into the following simple form

$$\sum_i \Re(x_{ii}) \frac{m_i}{v} = \sum_{i,j} |y_{ij}|^2. \quad (2)$$

The appearance of new operator contributions already at dimension five is a singular feature of effective theories with new light vector-like fermions and intrinsically connected to the resolution of the SM hierarchy problem within such scenarios. These dimension five contributions are thus expected to represent the dominant probe of new dynamics in the UV. At the same time one should keep in mind that unless the vector-like quarks are related to the SM field content by a symmetry, such cancelation of quadratic divergences is fine tuned in general. Furthermore, if one

*Electronic address:svjetlana.fajfer@ijs.si

†Electronic address:admir.greljo@ijs.si

‡Electronic address:jernef.kamenik@ijs.si

§Electronic address:ivana.mustac@ijs.si

considers the running of the leading vector-like quark operator and the SM couplings, even if tuned to cancel at one scale, the quadratic divergences will not cancel at other scales. Thus, the effective theory discussion concerning EW naturalness should be understood under the implicit assumption that the relation (2) is enforced by symmetry in the UV complete theory.

Furthermore, even though a (symmetry enforced) relation (2) removes the quadratic UV sensitivity of the Higgs potential, logarithmically divergent contributions remain present in the effective theory. The biggest resulting shift to the bare Higgs mass (δm_h) is now due to the new heavy quark states with bilinear couplings to the Higgs. Assuming a single such state (f) cancelling the one-loop quadratically divergent contribution to δm_h of the top quark, the dominant remaining correction is of the form

$$\delta m_h^2 \approx \frac{3m_t^2}{4\pi^2 v^2} m_f^2 \log \frac{\Lambda^2}{m_f^2}, \quad (3)$$

where the result was obtained using a hard UV cut-off of the loop momentum integral and equating it with the cut-off scale of the effective theory Λ . We immediately observe that allowing for only moderate fine-tuning (requiring conservatively $\delta m_h^2/m_h^2 \lesssim 10$) and the effective theory treatment valid (and thus $m_f \ll \Lambda$) requires f to be relatively light ($m_f \lesssim 1$ TeV).

Treating the Higgs as a composite field of a strongly interacting theory leads to the appearance of a number of dimension six operators affecting flavor, EW and Higgs observables (c.f. [5]). However, in models where the new vector-like quarks (possibly mixing with the chiral quark multiplets) and the Higgs are the lightest composite remnants of the strongly interacting sector, the dominant effects are expected from operators involving these fields. It is therefore meaningful to focus primarily on the leading dimension five contributions.¹ It turns out that they can always be parametrized in a way that preserves the form of gauge interactions of the renormalizable theory. Therefore the only way to approach and constrain such terms is by studying their impact on Higgs phenomenology, which is the main topic of the present work.²

The paper is structured as follows. In Sec. II we present some general considerations of models with vector-like quarks including generic flavor, electroweak and Higgs constraints on their interactions, stemming from renormalizable as well as leading dimension five non-renormalizable terms in the effective Lagrangian. Then in Secs. III – V we consider three specific model examples and analyze their viability in light of the derived direct and indirect constraints. For simplicity we will consider examples where vector-like quarks appear in existing weak representations of SM chiral quarks, thus allowing for kinetic mixing with chiral quark multiplets, with interesting phenomenological consequences. We summarize our conclusions in Sec. VI. Several supporting derivations and analyses of experimental constraints have been relegated to the appendices.

II. GENERAL CONSIDERATIONS

A. Renormalizable models

Since all vector-like quark models under consideration only contain colored fermions in SM gauge representations and charges, we can start by considering the mass matrices of the up- and down-type quarks in the weak (chiral) eigenbasis

$$-\mathcal{L}_{\text{mass}} = \bar{u}_L^i \mathcal{M}_u^{ij} u_R^j + \bar{d}_L^i \mathcal{M}_d^{ij} d_R^j + \text{h.c.}, \quad (4)$$

where the indices i, j run over all dynamical quark flavors (including new vector-like generations). The mass matrices $\mathcal{M}_{u,d}$ can be diagonalized via bi-unitary rotations as $\mathcal{M}_{u,d,\text{diag}} = U_L^{u,d} \mathcal{M}_{u,d} U_R^{u,d\dagger}$. Consequently, the gauge and Higgs interactions of physical quarks in the mass eigenbasis can be written in the general form (c.f. [8])

$$\mathcal{L}_W = -\frac{g}{\sqrt{2}} (V_{ij}^L \bar{u}^i \gamma^\mu P_L d^j + V_{ij}^R \bar{u}^i \gamma^\mu P_R d^j) W_\mu^+ + \text{h.c.}, \quad (5)$$

$$\mathcal{L}_Z = -\frac{g}{2c_W} (X_{ij}^u \bar{u}^i \gamma^\mu P_L u^j - X_{ij}^d \bar{d}^i \gamma^\mu P_L d^j + Y_{ij}^u \bar{u}^i \gamma^\mu P_R u^j - Y_{ij}^d \bar{d}^i \gamma^\mu P_R d^j - 2s_W^2 J_{\text{EM}}^\mu) Z_\mu, \quad (6)$$

$$\mathcal{L}_h^{(0)} = -(X_{ij}^u - Y_{ij}^u) \frac{m_j}{v} \bar{u}^i P_R u^j h - (X_{ij}^d - Y_{ij}^d) \frac{m_j}{v} \bar{d}^i P_R d^j h + \text{h.c.}, \quad (7)$$

¹ For a recent analysis of dimension six operator effects in composite Higgs scenarios without dynamical vector-like fermions see [6].

² For recent related studies in the context of explicit composite Higgs model realisations see [7].

where $P_{R,L} = (1 \pm \gamma_5)/2$, $g = 2m_W/v \simeq 0.65$ is the weak coupling, while $s_W \simeq \sqrt{0.23}$ and $c_W = \sqrt{1 - s_W^2}$ are the sine and cosine of the weak angle, respectively. $J_{\text{EM}}^\mu = (2\bar{u}^i \gamma^\mu u^i - \bar{d}^j \gamma^\mu d^j)/3$ is the EM quark current. The flavor matrices $V^{L,R}$, $X^{u,d}$ and $Y^{u,d}$ are all given in terms of $U_{L,R}^{u,d}$, in particular we can write $V_{ij}^L \equiv (U_L^d)_{jk}^* (U_L^u)_{ik}$, where the repeated index runs over all left-handed weak doublets, and $V_{ij}^R \equiv (U_R^d)_{jk}^* (U_R^u)_{ik}$, where the repeated index runs over all right-handed weak doublets. Then the (hermitian) flavor matrices entering neutral current and Higgs interactions are given simply by $X^u \equiv V^L V^{L\dagger}$, $X^d \equiv V^{L\dagger} V^L$, $Y^u \equiv V^R V^{R\dagger}$ and $X^d \equiv V^{R\dagger} V^R$. Thus, non-standard Higgs interactions in such renormalizable models with extra quarks are necessarily constrained by charged and neutral weak currents among the known three generations of quarks. For example, the departures of V^L from 3×3 unitary matrix and the appearance of a non-zero V^R are constrained by precisely measured tree level charged current processes. For example, $\sum_{j=d,s,b} |V_{ij}^L|^2 = 1 - \Delta_i^u \leq 1$ (for $i = u, c, t$) and $\sum_{j=u,c,t} |V_{ji}^L|^2 = 1 - \Delta_i^d \leq 1$ (for $i = d, s, b$) are constrained in absence of V^R as $\Delta_u^u < 0.001$ [9], $\Delta_c^u < 0.052$ [10], $\Delta_t^u < 0.13$ (see Appendix A for details), $\Delta_d^d < 0.01$, $\Delta_s^d < 0.08$ [10] and $\Delta_b^d < 1 - |V_{tb}^L|^2 < 0.15$ (see Appendix A for details). Note that in models with no extra up-type (down-type) quarks, $\Delta_i^d = \delta X_{ii}^d$ ($\Delta_i^u = \delta X_{ii}^u$), where $\delta X_{ii}^{u,d} \equiv 1 - X_{ii}^{u,d}$. The entries of V^R on the other hand, are also constrained at the tree-level by searches for right-handed charged currents (c.f. [11] for a recent analysis). Unfortunately, without information on the matrix elements involving also extra quarks present in the model beyond the known SM generations, these cannot be directly related to Z and Higgs couplings ($Y^{u,d}$).

In addition, one can obtain tree-level constraints on the off-diagonal entries of $X^{u,d}$ and $Y^{u,d}$ directly from their contributions to Z -mediated FCNCs of up- or down-type quarks. In all scenarios we consider, either nonstandard $X_{ij}^{u,d} \neq \delta_{ij}$ or $Y_{ij}^{u,d} \neq 0$ are generated but not both. In this case the bounds on non-diagonal entries of $X^{u,d}$ or $Y^{u,d}$ read $|X_{cu}^u|, |Y_{cu}^u| < 2.1 \times 10^{-4}$ [12, 13], $|X_{tu,tc}^u|, |Y_{tu,tc}^u| < 0.14$ (see Appendix A for details); $\text{Re}(X_{ds}^d), \text{Re}(Y_{ds}^d) < 1.4 \times 10^{-5}$, $|X_{db}^d|, |Y_{db}^d| < 4 \times 10^{-4}$ and $|X_{sb}^d|, |Y_{sb}^d| < 1 \times 10^{-3}$ (see Appendix B for details). Finally, electroweak measurements provide strong tree-level constraints also on the diagonal entries of $X^{u,d}$ and $Y^{u,d}$ corresponding to the five light quark flavours (see Appendix C for details).

The main consequence of the above discussion is that in renormalizable models with additional vector-like quarks, Higgs couplings to the known three generations of quarks, except possibly the top (i.e. X_{tt}^u, Y_{tt}^u), must remain SM-like, irrespective of the spectrum or interactions of additional heavy quarks. This is because they are rigidly related to the corresponding Z couplings, and thus subject to severe constraints from charged and neutral weak currents. In order to possibly obtain more interesting Higgs phenomenology, we are thus led to consider effects of higher-dimensional operators.

B. Including non-renormalizable Higgs interactions

Treating the SM as an effective field theory with particle content valid below a UV cut-off scale Λ , it is well known that the leading higher dimensional operators involving quark fields are of dimension six, a virtue of the chiral nature of weak interactions in the SM. Thus, effects of NP degrees of freedom appearing above Λ in low energy observables are suppressed by at least two powers of $1/\Lambda$. On the other hand, in presence of dynamical vector-like quarks, the leading non-renormalizable operators can appear already at dimension five. In general, they are of the form $H^\dagger H \bar{Q} Q$ and $H^\dagger H \bar{q} Q$, where q denotes the SM chiral quark multiplets.³ The main consequences of these new interactions are (i) direct di-Higgs coupling to physical quarks [x_{ij} in eq. (1)] with possible implications for the SM hierarchy problem; (ii) modifications of single Higgs - quark couplings [y_{ij} in eq. (1)] not related to weak neutral or charged currents. In the quark mass eigenbasis these additional contributions can generally be written as

$$\mathcal{L}_h^{(1)} = \left(\frac{X_{ij}^{u'}}{\Lambda} \bar{u}_L^i u_R^j + \frac{X_{ij}^{d'}}{\Lambda} \bar{d}_L^i d_R^j \right) \left[v h + \frac{h^2}{2} \right] + \text{h.c.}, \quad (8)$$

where Λ is the UV cut-off scale of the effective theory encompassing the SM together with a number of additional quark-like states. First note that the appearance of $X_{ij}^{u,d'}$ couplings of the known three generations of quarks to the Higgs is a manifestation of mixing between chiral and vector-like quarks, which is in general unrelated and thus

³ In the following we do not consider operators of the form $\bar{Q}(\sigma \cdot \mathcal{G})Q$ and $\bar{q}(\sigma \cdot \mathcal{G})Q$, where $\sigma_{\mu\nu} = i[\gamma_\mu, \gamma_\nu]/2$ and $\mathcal{G}_{\mu\nu} \in \{T^a G_{\mu\nu}^a, \tau^a W_{\mu\nu}^a, B_{\mu\nu}\}$ stands for the three SM gauge field strengths, since these are not directly related to Higgs phenomenology. If the vector-like quarks mix with the SM generations, they will induce anomalous dipole gauge interactions of SM quarks at order $1/m_Q \Lambda$, where m_Q is the vector-like quark mass scale, and can be constrained from precision electroweak, flavor and collider observables (c.f. [14]). Modulo fine-tuned cancelations in these constraints, their presence would thus not affect our analysis.

unconstrained by charged and neutral weak currents. On the other hand, naturalness of the hierarchical quark mass spectrum would require $|X_{ij}^u X_{ji}^{u*}| v^4 / \Lambda^2 < m_i m_j$ [15]. In order to keep our analysis as general as possible, we shall not impose such a condition on the parameter space of our models, although one should keep it in mind. The off-diagonal values of $X^{u,d}$ are constrained by low energy flavour observables [16]. In the up-sector, $|X_{uc,cu}^u| v / \Lambda < 7 \times 10^{-5}$ and $\sqrt{|X_{tu,tc}^u|^2 + |X_{ut,ct}^u|^2} v / \Lambda < 0.34$ are constrained by D^0 mixing and $t \rightarrow (c, u)h$ decay searches, respectively. Similarly, K^0 , B_d and B_s mixing measurements require $|X_{sd,ds}^d| v / \Lambda < 2 \times 10^{-5}$, $|X_{bd,db}^d| v / \Lambda < 2 \times 10^{-4}$ and $|X_{sb,bs}^d| v / \Lambda < 1 \times 10^{-3}$, respectively.⁴

Potentially the most striking tree-level effects on Higgs phenomenology in non-renormalizable vector-like quark models are thus modifications of the flavor diagonal Higgs couplings to lighter quarks. In particular, in the SM the total Higgs decay width is dominated by the $h \rightarrow b\bar{b}$ channel, the first hints of which have also been observed at the LHC [17, 18]. The modifications of y_{bb} in eq. (1) can thus have important consequences for all experimentally observed Higgs signals. Similarly, while the $h \rightarrow u\bar{u}, d\bar{d}, s\bar{s}$ or $h \rightarrow c\bar{c}$ decays are very suppressed in the SM and also cannot be reconstructed at the LHC due to the large QCD backgrounds, they can contribute to the total Higgs decay width in case of non-zero $X_{ii}^{u,d}$. In particular, defining $\Delta\gamma \equiv \sum_{f=d,u,s,c} \Gamma_{h \rightarrow f\bar{f}} / \Gamma_h^{\text{SM}}$, we obtain $\sum_{i=d,s} |X_{ii}^d v / \Lambda - m_i / v|^2 + \sum_{i=u,c} |X_{ii}^u v / \Lambda - m_i / v|^2 \simeq 10^{-3} \Delta\gamma$ showing that sizable enhancement in these decay channels is possible (although the required values of $X_{ii}^{u,d} / \Lambda$ would necessarily violate the corresponding quark mass naturalness conditions) and that a non-trivial constraint on $X_{ii}^{u,d}$ can in principle be obtained from the total Higgs decay width. This rises a question of importance of $\bar{u}u \rightarrow h$ (or to a lesser extent $\bar{d}d \rightarrow h$) production mechanism compared to the dominant $gg \rightarrow h$ mode at the LHC and Tevatron. In the zero-width approximation and at leading order in QCD, the ratio of the relevant hadronic cross sections in the two cases can be written as

$$\frac{\sigma(p_1 p_2 \rightarrow h)_{u\bar{u}}}{\sigma(p_1 p_2 \rightarrow h)_{gg}} = \frac{\Gamma(h \rightarrow \bar{u}u) \mathcal{L}_{p_1 p_2}^{u\bar{u}}(\tau)}{\Gamma(h \rightarrow gg) \mathcal{L}_{p_1 p_2}^{gg}(\tau)}, \quad (9)$$

where $\tau \equiv m_h^2 / s$ with s being the invariant collider energy squared. The relevant luminosity functions at hadronic ($p_1 p_2$) colliders are given by

$$\mathcal{L}_{p_1 p_2}^{q_1 q_2}(x) = \frac{1}{1 + \delta_{q_1 q_2}} \int_x^1 \frac{dy}{y} [f_{q_1}^{p_1}(y) f_{q_2}^{p_2}(x/y) + f_{q_1}^{p_2}(y) f_{q_2}^{p_1}(x/y)], \quad (10)$$

where $f_{q_j}^{p_i}$ are the corresponding parton distribution functions (pdfs). Using the LO MSTW2008 [19] set, with the factorization and renormalization scales fixed to $m_h \simeq 125$ GeV, the ratio $\mathcal{L}_{pp}^{u\bar{u}} / \mathcal{L}_{pp}^{gg}$ for $\sqrt{s} = 7$ TeV and $\sqrt{s} = 14$ TeV is 3.9% and 2.3% respectively.⁵ Thus, even assuming comparable $h \rightarrow u\bar{u}$ and $h \rightarrow gg$ decay rates, the up-quark contribution to Higgs production at the LHC is below the $\sim 12\%$ theoretical uncertainties [20] of the dominant gluon fusion production cross section. Conversely, at the Tevatron, we find the relevant ratio $\mathcal{L}_{pp}^{u\bar{u}} / \mathcal{L}_{pp}^{gg}$ for $\sqrt{s} = 1.96$ TeV to be sizable 26%. However, given the low statistics in the gluon fusion Higgs production channel at the Tevatron [21], this again gives no relevant constraint on $\Gamma(h \rightarrow \bar{u}u)$. In the future, enhanced di-Higgs production at the LHC could possibly offer a competitive constraint on X_{uu}^u / Λ . In particular, the relevant LO hadronic cross section is given by

$$\sigma(p_1 p_2 \rightarrow hh)^{X'} = \int_{4\tau}^1 dx \hat{\sigma}_{u\bar{u} \rightarrow hh}^{X'}(xs) \mathcal{L}_{p_1 p_2}^{u\bar{u}}(x), \quad (11)$$

where

$$\hat{\sigma}_{u\bar{u} \rightarrow hh}^{X'}(\hat{s}) = \frac{|X_{uu}^u|^2 \beta_h}{64\pi\Lambda^2} \left(1 + \frac{3m_h^2}{\hat{s} - m_h^2} \right)^2, \quad (12)$$

and $\beta_h = \sqrt{1 - 4m_h^2 / \hat{s}}$. Using the same pdf parameters as above we obtain $\sigma(pp \rightarrow hh)^{X'} / [(|X_{uu}^u| / 0.03)(1\text{TeV}/\Lambda)]^2 \simeq 5(11)$ fb at the 8 TeV (14 TeV) LHC, compared to the SM LO predictions [22] of $\sigma(pp \rightarrow hh)^{\text{SM}} = 4(16)$ fb, respectively.

⁴ All bounds from neutral meson mixing apply in absence of large cancellations with the tree-level Z-mediated $X^{u,d}, Y^{u,d}$ contributions.

⁵ Using instead the NNLO MSTW2008 pdfs with the same scale choices yields ratios of 4.0% and 2.5% respectively.

C. Impact of existing Higgs data

Most interesting effects involving light vector-like quarks in Higgs phenomenology appear at the one-loop level. In general, Higgs-fermion interactions of the form (1) will contribute to gluon fusion production and di-photon decay of the Higgs at one loop

$$R_{gg} \equiv \frac{\Gamma_{h \rightarrow gg}}{\Gamma_{h \rightarrow gg}^{SM}} \simeq \frac{\left| \sum_i y_{ii} \frac{v}{m_i} C(r_i) F_{1/2}(\tau_i) \right|^2}{\left| \frac{1}{2} F_{1/2}(\tau_t) + \frac{1}{2} F_{1/2}(\tau_b) \right|^2}, \quad (13)$$

$$R_{\gamma\gamma} \equiv \frac{\Gamma_{h \rightarrow \gamma\gamma}}{\Gamma_{h \rightarrow \gamma\gamma}^{SM}} \simeq \frac{\left| F_1(\tau_W) + \sum_i y_{ii} \frac{v}{m_i} d(r_i) Q_i^2 F_{1/2}(\tau_i) \right|^2}{\left| F_1(\tau_W) + \frac{4}{3} F_{1/2}(\tau_t) \right|^2}, \quad (14)$$

where $d(r_i)$ and $C(r_i)$ are the dimension and index of the color representation of f_i , respectively, and Q_i is its electric charge. The relevant loop functions $F_1(\tau)$ and $F_{1/2}(\tau)$ can be found e.g. in ref. [23], and $\tau_i \equiv m_h^2/(4m_i^2)$. In the limit of large fermion mass, $F_{1/2}(\tau) \rightarrow F_{1/2}(0) = 4/3$. In the SM, gluon fusion production, $gg \rightarrow h$, is dominated by the top quark loop with $(1/2)F_{1/2}(\tau_t) = 0.688$, with minor contribution from the bottom quark $(1/2)F_{1/2}(\tau_b) = -0.04 + i0.06$. Conversely, Higgs decay to two photons in the SM is dominated by the W boson loop yielding $F_1(\tau_W) = -8.34$, and interfering destructively with the top quark contribution of $(4/3)F_{1/2}(\tau_t) = 1.84$. It turns out that lighter quark contributions to loop induced Higgs processes are negligible even if their couplings to the Higgs saturate the limits from $\Delta\gamma$ as discussed below.

In order to evaluate the current constraints on modified Higgs interactions, we analyze the latest available Higgs data, presented in Table I. Our procedure follows closely those of similar previous analyses [24] and we refer the reader to those references for a detailed discussion of the current issues in using the data set.

Measurements are given in terms of Higgs signal strengths normalized to SM predictions

$$\mu_{A \rightarrow h}^{h \rightarrow B} = \frac{\sigma_{A \rightarrow h} \mathcal{B}_{h \rightarrow B}}{\sigma_{A \rightarrow h}^{SM} \mathcal{B}_{h \rightarrow B}^{SM}}, \quad (15)$$

where $A \rightarrow h$ and $h \rightarrow B$ stands for different production mode and decay channel, respectively. Experimental best-fit values and variances are denoted by $\hat{\mu}_i$ and $\hat{\sigma}_i^2$, respectively. Experimental collaborations generally provide plots with separate contribution from VBF plus VH, and from ggF plus ttH production channels for a given decay channel. In this case, we take into account their correlation, obtaining a correlation parameter ρ by reproducing the plots. The contribution from these decay channels to the total χ^2 function is

$$\chi_1^2 = \sum_i \left(\mu_{GF}^i - \hat{\mu}_{GF}^i, \mu_{VF}^i - \hat{\mu}_{VF}^i \right) \begin{pmatrix} (\hat{\sigma}_{GF}^i)^2 & \rho^i \hat{\sigma}_{GF}^i \hat{\sigma}_{VF}^i \\ \rho^i \hat{\sigma}_{GF}^i \hat{\sigma}_{VF}^i & (\hat{\sigma}_{VF}^i)^2 \end{pmatrix}^{-1} \begin{pmatrix} \mu_{GF}^i - \hat{\mu}_{GF}^i \\ \mu_{VF}^i - \hat{\mu}_{VF}^i \end{pmatrix}, \quad (16)$$

where GF stands for ggF+ttH, and VF stands for VBF+VH, and index i runs over decay channels.⁶ If the separation into production modes is not provided, we use the data from different search categories for a particular decay channel, which generally target certain production mechanism, but does not imply 100% purity. Inclusive categories are dominated by ggF ($\sim 90\%$), while VBF-tagged categories can have 20% to 50% contamination from ggF. VH- and ttH-tagged categories are assumed to be pure. In this case, we write

$$\frac{\sigma_{A \rightarrow h}}{\sigma_{A \rightarrow h}^{SM}} = \xi_{ggF} \frac{\sigma_{ggF}}{\sigma_{ggF}^{SM}} + \xi_{VBF} \frac{\sigma_{VBF}}{\sigma_{VBF}^{SM}} + \xi_{VH} \frac{\sigma_{VH}}{\sigma_{VH}^{SM}} + \xi_{ttH} \frac{\sigma_{ttH}}{\sigma_{ttH}^{SM}}, \quad (17)$$

where ξ_i represent contributions of the specified production mechanisms for the given category. We do not assume correlations here, and add each search category to χ^2 separately,

$$\chi_2^2 = \sum_j \left(\frac{\mu_j - \hat{\mu}_j}{\hat{\sigma}_j} \right)^2, \quad (18)$$

⁶ ttH contribution in GF is less than 1%.

| Decay channel | Production mode | Signal strength | Comment |
|------------------------------|---------------------|-----------------|--------------------------------------|
| ATLAS | | | |
| $h \rightarrow ZZ^*$ | Inclusive (87% ggF) | 1.5 ± 0.4 | [17, 25] |
| $h \rightarrow b\bar{b}$ | VH | -0.4 ± 1.0 | [17] |
| $h \rightarrow WW^*$ | ggF+ttH | 0.79 ± 0.35 | Correlation $\rho = -0.3$, [17, 26] |
| | VBF+VH | 1.6 ± 0.8 | |
| $h \rightarrow \gamma\gamma$ | ggF+ttH | 1.60 ± 0.44 | Correlation $\rho = -0.4$, [17, 27] |
| | VBF+VH | 1.80 ± 0.87 | |
| $h \rightarrow \tau\tau$ | ggF+ttH | 2.2 ± 1.6 | Correlation $\rho = -0.5$, [17] |
| | VBF+VH | -0.3 ± 1.1 | |
| CMS | | | |
| $h \rightarrow b\bar{b}$ | VH | 1.3 ± 0.7 | [18] |
| $h \rightarrow WW^*$ | 0/1 jet (97% ggF) | 0.76 ± 0.21 | [28] |
| | VBF-tag (20% ggF) | 0.0 ± 0.7 | [18] |
| | VH | -0.3 ± 2.1 | [18] |
| $h \rightarrow ZZ^*$ | ggF+ttH | 0.90 ± 0.45 | Correlation $\rho = -0.7$, [29] |
| | VBF+VH | 1.0 ± 2.3 | |
| $h \rightarrow \gamma\gamma$ | ggF+ttH | 0.52 ± 0.40 | Correlation, $\rho = -0.5$, [30] |
| | VBF+VH | 1.5 ± 0.9 | |
| $h \rightarrow \tau\tau$ | 0/1 jet (80% ggF) | 0.73 ± 0.51 | [31] |
| | VBF-tag (20% ggF) | 1.37 ± 0.63 | [31] |
| | VH | 0.75 ± 1.5 | [31] |

Table I: LHC Higgs data used in the analysis.

and the total χ^2 function is given by $\chi^2 = \chi_1^2 + \chi_2^2$.

We take into account the recent evaluation [20] of ggF production in the SM at approximate N³LO in perturbative expansion, which exhibits a 17% shift with respect to the values adopted by experimental collaborations, by rescaling central values for signal strengths which depend on ggF production by a factor $1/(1+0.17\xi_{ggF})$. On the other hand, we have checked that the resulting slightly reduced theory error (from 14% to 12%) has negligible effect on the reported variances. Finally, we note that using 7 TeV and 8 TeV data combinations introduces potentially non-negligible effects due to the different parton luminosities when constraining NP. We expect however these to be subleading compared to the overall theoretical uncertainty, especially in light of our ignorance of higher order QCD effects in NP contributions.

In the following, we present results of our analysis. The SM is in overall very good agreement with the data. The associated χ^2 for 19 observables presented in Table I is $\chi_{SM}^2 = 16.2$ corresponding to a p-value of 0.64. Within the vector-like quark scenarios, all the modifications to Higgs signal strengths can be expressed in terms of four parameters, R_{gg} , $R_{\gamma\gamma}$, R_{bb} and $\Delta\gamma$, where

$$R_{bb} \equiv \frac{\Gamma_{h \rightarrow b\bar{b}}}{\Gamma_{h \rightarrow b\bar{b}}^{SM}} = \left(\frac{|y_{bb}|v}{m_b} \right)^2. \quad (19)$$

In particular, one can write

$$\mu_{GF}^{h \rightarrow \gamma\gamma} = \frac{R_{gg}}{\hat{\Gamma}} R_{\gamma\gamma}, \quad \mu_{GF}^{h \rightarrow ZZ, WW, \tau\tau} = \frac{R_{gg}}{\hat{\Gamma}}, \quad \mu_{VF}^{h \rightarrow \gamma\gamma} = \frac{R_{\gamma\gamma}}{\hat{\Gamma}}, \quad \mu_{VF}^{h \rightarrow ZZ, WW, \tau\tau} = \frac{1}{\hat{\Gamma}}, \quad \mu_{VH}^{h \rightarrow b\bar{b}} = \frac{R_{bb}}{\hat{\Gamma}}. \quad (20)$$

The modification of the total Higgs decay width coming from R_{gg} , R_{bb} and $\Delta\gamma$ is taken into account by writing

$$\hat{\Gamma} \equiv \frac{\Gamma_{tot}}{\Gamma_{tot}^{SM}} = 0.569R_{bb} + 0.317 + 0.085R_{gg} + \Delta\gamma, \quad (21)$$

where $\Delta\gamma$ is constrained to $\Delta\gamma > 0$.

We consider four different scenarios, with different choices of the fitting parameters. In each case, the best-fit point is determined by minimizing the χ^2 function. Results are presented in the $(R_{gg}, R_{\gamma\gamma})$ plane, after marginalizing over the other parameters. We define 68.2% (1σ) best-fit region to satisfy $\chi_{min}^2 < \chi^2 < \chi_{min}^2 + 2.3$, and 95.5% (2σ) best-fit region to satisfy $\chi_{min}^2 + 2.3 < \chi^2 < \chi_{min}^2 + 6.2$.

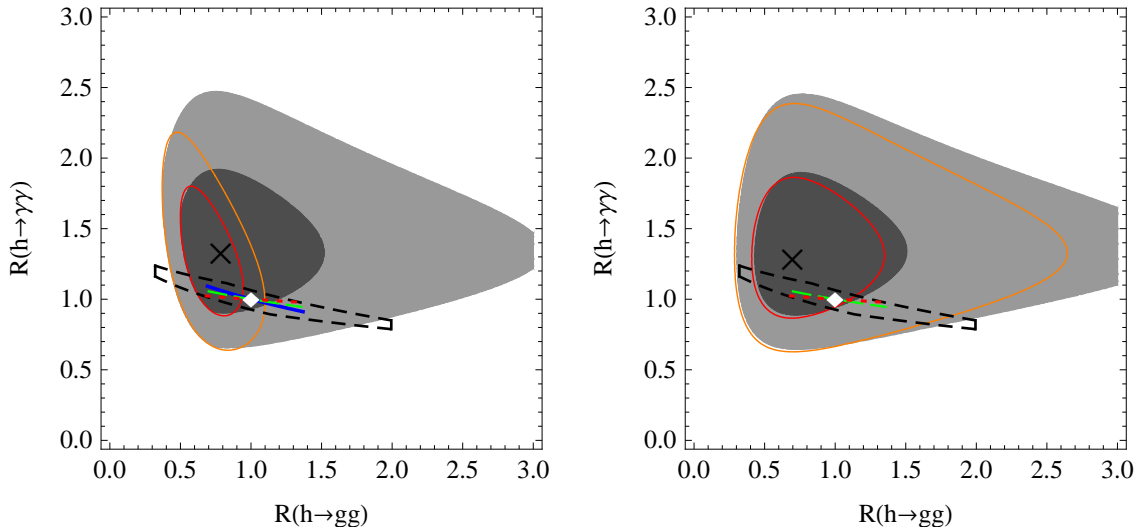


Figure 1: **Left:** Fit of Higgs data taking $R_{gg} \equiv R(h \rightarrow gg)$, $R_{\gamma\gamma} \equiv R(h \rightarrow \gamma\gamma)$ and $\Delta\gamma$ as fitting parameters. The best fit point (cross), 1σ (dark gray) and 2σ (light gray) regions are shown in the $(R_{gg}, R_{\gamma\gamma})$ plane after marginalizing over $\Delta\gamma$. The SM reference scenario is marked with a diamond. Results of the fit for $\Delta\gamma$ fixed to its SM value are given by the darker red contour (1σ region) and the lighter orange contour (2σ region). The resulting prediction from the non-renormalizable model with an additional up-like vector-like quark, the model with a down-like vector-like and the model with a doublet vector-like quark in the no-mixing and negligible isospin breaking limit are given by the continuous-blue, dotted-red and dashed-green curves, respectively. General predictions from the non-renormalizable model with a doublet vector-like quark are given by the region presented with the dashed-black contour (see text for details). **Right:** Fit of Higgs data taking R_{gg} , $R_{\gamma\gamma}$, R_b and $\Delta\gamma$ as fitting parameters. The best fit point (cross), 1σ (dark gray) and 2σ (light gray) regions are shown in the $(R_{gg}, R_{\gamma\gamma})$ plane after marginalizing over R_b and $\Delta\gamma$. Results of the fit for $\Delta\gamma$ fixed to its SM value are given by the darker red contour (1σ region) and the lighter orange contour (2σ region). The resulting prediction from the non-renormalizable model with a down-like vector-like and the model with a doublet vector-like quark in the no-mixing and negligible isospin breaking limit are given by dotted-red and dashed-green curves, respectively. General predictions from the non-renormalizable model with a doublet vector-like quark are given by the region presented with the dashed-black contour (see text for details).

First, we take R_{gg} and $R_{\gamma\gamma}$ as fitting parameters, while fixing R_{bb} and $\Delta\gamma$ to their SM values. This applies to scenarios, where the couplings of SM quarks to the Higgs (the Yukawas) are not modified, while R_{gg} and $R_{\gamma\gamma}$ receive new loop contributions. In models with vector-like quarks this corresponds to the limit of zero mixing between the chiral and vector-like quarks. The minimum of the χ^2 corresponds to a point $(R_{gg}, R_{\gamma\gamma}) = (0.71, 1.30)$ with $\chi_{min}^2 = 12.7$ and p-value 0.76. Second, we take R_{gg} , $R_{\gamma\gamma}$ and $\Delta\gamma$ as fitting parameters, while fixing $R_{bb} = 1$. This corresponds to scenarios where the vector-like quarks do not mix with the b quark, but possibly with the lighter quark generations (see [32] for a recent model example). In this case, the point $(R_{gg}, R_{\gamma\gamma}, \Delta\gamma) = (0.79, 1.33, 0.12)$ corresponds to the minimum of the χ^2 , with $\chi_{min}^2 = 12.6$ and p-value 0.7. The results for the first two scenarios are presented on the left plot in Fig. 1. For the first scenario, 1σ and 2σ contours are represented by (darker) red and (lighter) orange curves, respectively.

In the third case, we take R_{gg} , $R_{\gamma\gamma}$ and R_{bb} as fitting parameters, while fixing $\Delta\gamma$ to its SM value. This case applies to the most studied scenarios in the literature, where the vector-like quarks only mix with the third generation (c.f. [33] for a recent study). The minimum of the χ^2 corresponds to a point $(R_{gg}, R_{\gamma\gamma}, R_{bb}) = (0.70, 1.29, 0.97)$ with $\chi_{min}^2 = 12.7$ and p-value 0.69. In the last case, we take all four parameters to fit the data, corresponding to the most general case of vector-like quarks mixing with all three SM generations. Here, the minimum of the χ^2 corresponds to a point $(R_{gg}, R_{\gamma\gamma}, R_{bb}, \Delta\gamma) = (0.73, 1.31, 0.74, 0.2)$ with $\chi_{min}^2 = 12.4$ and p-value 0.65. The results for the last two scenarios are presented on the same plot, Fig. 1 right. For the third scenario, 1σ and 2σ contours are represented by (darker) red and (lighter) orange curves, respectively.

The main observation at this point is that allowing for a modification of R_{bb} and/or $\Delta\gamma$ (non-zero mixing of vector-like quarks with some of the SM chiral quarks) significantly increases the allowed range of R_{gg} , while it has much less of an effect on $R_{\gamma\gamma}$. This has important implications for constraining vector-like quark models using Higgs data, since these generically predict much larger effects in R_{gg} . In the following sections we apply these general results to a few simplest SM extensions with a single light vector-like quark state below the effective theory cut-off Λ .

III. SINGLET UP-TYPE VECTOR-LIKE QUARK

A. Renormalizable model

As a first example, we consider the SM extended by a vector-like quark pair (U_L, U_R) in the $\mathbf{1}_{2/3}$ representation of the SM electroweak group. In the most general renormalizable model the quark Yukawa interactions and mass terms can be described by the following Lagrangian

$$-\mathcal{L}_U^{(0)} = y_d^{ij} \bar{q}_L^i H d_R^j + y_u^{ij} \bar{q}_L^i \tilde{H} u_R^j + y_U^i \bar{q}_L^i \tilde{H} U_R + M_U \bar{U}_L U_R + \text{h.c.}, \quad (22)$$

where $\tilde{H} \equiv i\tau_2 H^*$, $H = (G^+, (v + h + iG_0)/\sqrt{2})$ is the SM Higgs doublet, q_L^i the SM quark doublets and u_R^i the SM up-type quark singlets. Note that additional kinetic mixing terms of the form $\bar{U}_L u_R^i$ can always be rotated away and reabsorbed into the definitions of $y_{u,U}$. Furthermore, one can, without loss of generality, choose a weak interaction basis where y_u is diagonal and real. After EW symmetry breaking (EWSB) the mass matrices for up- and down-type quarks are

$$\mathcal{M}_u = \begin{pmatrix} y_u v/\sqrt{2} & y_U v/\sqrt{2} \\ 0 & M_U \end{pmatrix}, \quad \mathcal{M}_d = (y_d v/\sqrt{2}). \quad (23)$$

The weak gauge and Higgs interactions of 4 (u, c, t, u') physical up-like and 3 (d, s, b) down-like quarks in this (mass) eigenbasis are given by eqs. (5)-(7), where $V^R = 0$, V^L is a general 4×3 matrix and $X^d = \mathbb{I}_{3 \times 3}$. Note that in this model $X_{ii}^u = 1 - \Delta_i^u$ and that tree level constraints on the entries of X^u already severely constrain the admixture of U within the physical u and c quarks. In particular, we find for the 3×3 sub-matrix of X^u describing Z and Higgs couplings to known up-type quark flavours

$$|X^u - \mathbb{I}|_{3 \times 3} < \begin{bmatrix} 0.001 & 2.1 \times 10^{-4} & 0.14 \\ & 0.0026 & 0.14 \\ & & 0.13 \end{bmatrix}. \quad (24)$$

Loop-level u' effects provide better constraints only on the mixing of the vector-like singlet quark with the top quark. Neglecting the small mixing with the first two generations (effectively setting $y_U^{u,c} = 0$) the $t - u'$ system can be described by three independent physical parameters: two quark masses $(m_t, m_{u'})$ and a single (left-handed) mixing angle (θ_{tU}) , which are defined as [34]

$$\tan(2\theta_{tU}) = \frac{\sqrt{2} v y_U^t M_U}{M_U^2 - [(y_u^t)^2 + (y_U^t)^2] v^2/2}, \quad (25)$$

$$m_t m_{u'} = M_U y_u^t \frac{v}{\sqrt{2}}, \quad m_t^2 + m_{u'}^2 = M_U^2 + \frac{v^2}{2} [(y_u^t)^2 + (y_U^t)^2]. \quad (26)$$

In terms of these, $X_{tt}^u = c_{tU}^2$, $X_{t'u'}^u = c_{tU} s_{tU}$ and $X_{t'U}^u = s_{tU}^2$, where $c_{tU} \equiv \cos \theta_{tU}$ and $s_{tU} \equiv \sin \theta_{tU}$.

Presently, the most sensitive observable to nonzero s_{tU} is the ρ parameter, which receives a new contribution of the form [34]

$$\Delta\rho = \frac{\alpha N_C}{16\pi s_W^2} \frac{m_t^2}{m_W^2} s_{tU}^2 \left[-(1 + c_{tU}^2) + s_{tU}^2 r + 2c_{tU}^2 \frac{r}{r-1} \log(r) \right], \quad (27)$$

where $r \equiv m_{u'}^2/m_t^2$ and we have neglected terms of higher order in $m_{Z,b}^2/m_{t,u'}^2$. A comparison with the experimental bound of $\Delta\rho^{\text{exp}} = 4_{-4}^{+3} \times 10^{-4}$ [10] yields a constraint on s_{tU} as a function of the u' mass as shown in Fig. 2.

While the modified top quark coupling to the Higgs boson and the presence of an additional heavy quark can in principle impact also loop induced Higgs decays, namely $h \rightarrow gg$, $h \rightarrow \gamma\gamma$ and $h \rightarrow Z\gamma$, taking into account the above constraints on X_{ij}^u these effects turn out severely suppressed making it impossible in practice to distinguish the renormalizable model with a singlet vector-like up type quark from the SM in single Higgs production processes.

B. Non-renormalizable models

Extending the above renormalizable model with the leading dimension five operators containing the light SM fields and $U_{L,R}$ as the only dynamical degrees of freedom below a UV cut-off scale Λ , Yukawa interactions and mass terms

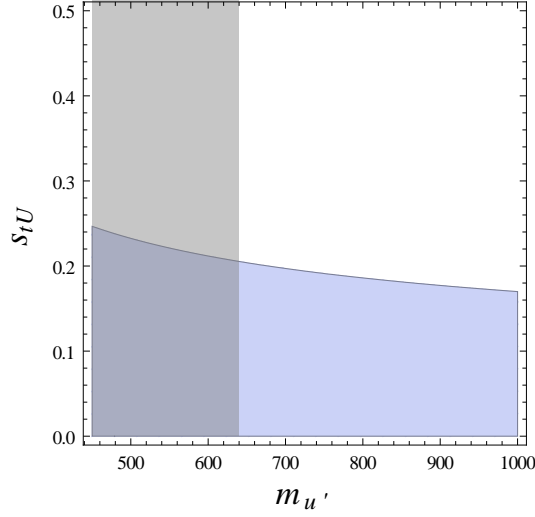


Figure 2: Upper limit at 95% C.L. on $t - u'$ (left-handed) mixing angle as a function of the u' quark mass in the model with an up-like vector-like quark. The gray region marks the ATLAS experimental search bound on the renormalizable model using the $u' \rightarrow th$ decay signature [35].

in eq. (22) receive corrections which result in modified interactions between up-type quarks and the Higgs. One can manifestly preserve the exact mass diagonalization procedure of the renormalizable model by parametrizing the leading non-renormalizable contributions in terms of the replacement

$$M_U \rightarrow M_U + c_2 \frac{v^2/2 - |H|^2}{\Lambda}, \quad (28)$$

plus an additional Higgs-dependent ‘kinetic mixing’ operator

$$-\mathcal{L}_U^{(1)} = c_1^i \frac{v^2/2 - |H|^2}{\Lambda} \bar{U}_L u_R^i. \quad (29)$$

After EWSB, the flavor structure of gauge interactions (and the associated bounds on X_{ij}^u) in the renormalizable model is preserved and only the Higgs interactions in the mass eigenbasis receive new contributions of the form (8) where $X^{d'} = 0$ (leading to $R_{bb} = 1$) while $X^{u'} = U_L^u \cdot [(0, 0), (c_1, c_2)] \cdot U_R^{u'\dagger}$. Interestingly, even though $X^{u'}$ has no observable effects on charged current interactions of quarks, one can derive an indirect bound on the diagonal entries of $X^{u'}$ from CKM unitarity. Following its definition, $X_{ij}^{u'} = (U_L^u)_{i4} (c_1^k (U_R^u)_{jk}^* + c_2 (U_R^u)_{j4}^*)$, we note that $|X_{ij}^{u'}|^2$ is proportional to $|(U_L^u)_{i4}|^2 = 1 - X_{ii}^u$, multiplied by at most $\mathcal{O}(1)$ coefficients in the effective field theory expansion c_1^i, c_2 and the unitary rotation U_R^u . Furthermore, the general identity $|(U_R^u)_{i4}|^2 = (m_i/M_U)^2 |(U_L^u)_{i4}|^2$ implies that c_2 contributions to u, c interactions are severely suppressed. Consequently, CKM unitarity constraints on $X_{uu,cc}^u$ yield indirect bounds on the diagonal elements $|X_{uu}^{u'}| \lesssim 0.03 \max(c_1^i)$ and $|X_{cc}^{u'}| \lesssim 0.2 \max(c_1^i)$. Note that sizable contributions to $\Delta\gamma$ are well consistent with these indirect CKM unitarity constraints.

The relevant modifications to R_{gg} and $R_{\gamma\gamma}$ in the up-type singlet scenario come from the modified top quark coupling and the presence of the additional heavy quark in the loop. In the limit $m_{t,u'} \gg m_h$, which is a good approximation here, the relevant numerical expressions are given by

$$R_{gg} = \frac{|0.68r_y - 0.040|^2 + 0.057^2}{0.65^2}, \quad R_{\gamma\gamma} = \frac{|-8.3 + 1.8r_y|^2}{|-6.5|^2}, \quad (30)$$

where to order $1/\Lambda$ and including possible small $t - u'$ mixing

$$r_y \equiv y_{tt} \frac{v}{m_t} + y_{u'u'} \frac{v}{m_{u'}} = 1 + s_{tU} (c_1^t c'_{tU} - c_2 s'_{tU}) \frac{v^2}{\Lambda m_t} - c_{tU} (c_1^t s'_{tU} + c_2 c'_{tU}) \frac{v^2}{\Lambda m_{u'}}. \quad (31)$$

Above we have used the short-hand notation for $c'_{tU} = \cos \theta'_{tU}$, $s'_{tU} = \sin \theta'_{tU}$, where the (right-handed) mixing angle θ'_{tU} is defined via $\tan \theta'_{tU} = (m_t/m_{u'}) \tan \theta_{tU}$. Thus, $h \rightarrow \gamma\gamma$ and $h \rightarrow gg$ are highly correlated in this set-up. Note

that at the one loop level and in the large $m_{t,u'}$ limit, contributions of renormalizable interactions of t and u' cancel exactly⁷, therefore, leading effects appear at order $\mathcal{O}(v/\Lambda)$.

The resulting predictions in the up-type singlet scenario are presented by the continuous (blue) curve in the $(R_{gg}, R_{\gamma\gamma})$ plain in left plot of Fig. 1. For concreteness we take $|(c_1^t, c_2^t)|/\Lambda \leq 1 \text{ TeV}^{-1}$ and $m_{u'} \geq 640 \text{ GeV}$ as suggested by direct searches [35] (see also the related discussion at the end of this section). Also, we take the $t - u'$ mixing angle to be within the 95% C.L. experimental bound discussed above ($s_{tU} \lesssim 0.2$). From the fit to Higgs data we obtain the preferred parameter ranges for r_y at 68% C.L. of $r_y = 0.86_{-0.09}^{+0.16}$ (when marginalizing over $\Delta\gamma$) and $r_y = 0.87 \pm 0.08$ (when fixing $\Delta\gamma = 0$). Interestingly, in both cases the fit slightly prefers $r_y < 1$. We note in passing that after marginalising over r_y in this scenario $\Delta\gamma$ is bounded as $\Delta\gamma < 0.75$ at 95% C.L., which in term implies $|X_{uu'}^{u'} + X_{cc'}^{u'}|v/\Lambda < 0.022$.

Finally, turning to the naturalness condition in (2), for the case of a single vector-like up-type singlet quark mixing with the top it reads

$$\frac{m_t^2 c_{tU}^2 + m_{u'}^2 s_{tU}^2}{v^2} = \frac{1}{\Lambda} [m_t s_{tU} (-c_1^t c'_{tU} + c_2 s'_{tU}) + m_{u'} c_{tU} (c_1^t s'_{tU} + c_2 c'_{tU})] + \mathcal{O}(1/\Lambda^2). \quad (32)$$

In the zero-mixing limit this leads to the prediction $r_y = 1 - (m_t/m_{u'})^2$, independent of the cut-off scale Λ . Interestingly, present Higgs data (exhibiting a preference for $r_y < 1$) are perfectly consistent with the naturalness condition. On the other hand, the Higgs fit results can also be interpreted in this context as imposing an indirect bound on the u' mass of $m_{u'} > 360 \text{ GeV}$ at 95% C.L.⁸

It is instructive to compare the above constraint to results of direct experimental searches for up-type singlet vector-like quarks. Interestingly, the most severe bound on u' in the renormalizable model and assuming dominant but small u' mixing with the top, $m_{u'} > 640 \text{ GeV}$ [35] is given by the ATLAS experimental search using the $u' \rightarrow th$ decay signature. In the non-renormalizable model the relevant couplings are given by $y_{tu'} = s_{tU} c_{tU} m_{u'}/v + s_{tU} (s'_{tU} c_1^t + c'_{tU} c_2)v/\Lambda$ and $y_{u't} = s_{tU} c_{tU} m_t/v - c_{tU} (c'_{tU} c_1^t - s'_{tU} c_2)v/\Lambda$. It is then easy to check that compared to $u' \rightarrow tZ$ and $u' \rightarrow bW$ rates, the $1/\Lambda$ corrections can in principle enhance the $\mathcal{B}(u' \rightarrow th)$ in the small s_{tU} limit (in the extreme case $\mathcal{B}(u' \rightarrow th) = 1$ the present bound is then strengthened to $m_{u'} \gtrsim 850 \text{ GeV}$ [35]) but cannot reduce it significantly below its value in the renormalizable model. However, if u' does not dominantly decay to third generation quarks (but instead to first two quark generations), the current direct search constraints are relaxed dramatically (c.f. [38]) and $m_{u'} \simeq 300 \text{ GeV}$ becomes a possibility. In summary, the Higgs fit already provides an interesting complementary constraint on scenarios with an up-type singlet vector-like quark cancelling the top-loop quadratic divergence to the Higgs mass. Although it is at present only marginally competitive with existing direct search bounds, it is far less sensitive to the hierarchy of mixings with the known three generations of up-type quarks (provided they are small).

IV. SINGLET DOWN-LIKE VECTOR-LIKE QUARK

A. Renormalizable model

Next we consider a SM extension with a vector-like quark pair (D_L, D_R) in the $\mathbf{1}_{-1/3}$ electroweak representation. The most general renormalizable Lagrangian now contains the Yukawa and mass terms

$$-\mathcal{L}_D^{(0)} = y_d^{ij} \bar{q}_L^i H d_R^j + y_u^{ij} \bar{q}_L^i \tilde{H} u_R^j + y_D^i \bar{q}_L^i H D_R + M_D \bar{D}_L D_R + \text{h.c.} \quad (33)$$

The mass matrices of up- and down-type quarks after EWSB have the form (23) with the replacement $u \leftrightarrow d$ and $U \leftrightarrow D$. In the mass-eigenbasis of 4 (d, s, b, d') physical down-type and 3 (u, c, t) up-type quarks the weak gauge and Higgs interactions are controlled by the general 3×4 matrix V_{ij}^L (again $V^R = 0$) defined as before leading to $X^u = \mathbb{1}_{3 \times 3}$. On the other hand, now the entries of the hermitian matrix X^d are experimentally severely constrained by their tree-level contributions to CKM non-unitarity and FCNCs in the down-quark sector and already preclude

⁷ Deviations from the large mass limit, as well as higher order perturbative corrections can upset this cancellation. However a recent study of gluon fusion production in the renormalizable model with a singlet vector-like top partner at NNLO in QCD [34] has found such effects to be tiny, only a few percent for maximal mixing.

⁸ For a comparison with the situation after the first Higgs data see [36].

significant mixing of the vector-like down-type singlet quark with any of the SM quark generations

$$|X^d - \mathbb{I}|_{3 \times 3} < \begin{bmatrix} 0.004 & 1.4 \times 10^{-5} & 4 \times 10^{-4} \\ & 0.006 & 0.001 \\ & & 0.0057 \end{bmatrix}. \quad (34)$$

We immediately observe that Higgs phenomenology in the renormalizable down-type singlet model is again indistinguishable from the SM. In particular, considering only the dominant effects due to $b-d'$ mixing and thus parametrizing $X_{bb}^d = c_{bD}^2$, $X_{bd'}^d = c_{bD}s_{bD}$ and $X_{d'd'}^d = s_{bD}^2$, where $c_{bD}^2 + s_{bD}^2 = 1$, experimental constraints indicate $s_{bD} = 0.05(4)$ (see Appendix C). This leads to maximum allowed relative deviations from SM predictions for the decay channels $h \rightarrow b\bar{b}$, $h \rightarrow gg$ and $h \rightarrow \gamma\gamma$ of 0.4%, 0.5% and -0.02% , respectively.

B. Non-renormalizable models

The leading higher dimensional modifications of Higgs interactions can again be most conveniently parametrized via the replacement

$$M_D \rightarrow M_D + c_2 \frac{v^2/2 - |H|^2}{\Lambda}, \quad (35)$$

plus an additional Higgs-dependent ‘kinetic mixing’ operator

$$-\mathcal{L}_D^{(1)} = c_1^i \frac{v^2/2 - |H|^2}{\Lambda} \bar{D}_L d_R^i, \quad (36)$$

yielding new Higgs interactions in the mass eigenbasis of the form (8), where now $X^{u'} = 0$ and $X^{d'} = U_L^d \cdot [(0, 0), (c_1, c_2)] \cdot U_R^{d'}$. Constraints on $|(U_L^d)_{4i}|^2 = 1 - X_{ii}^d$ lead to the following indirect bounds $|X_{dd'}^{d'}| \lesssim 0.06 \max(c_1^i)$, $|X_{ss}^{d'}| \lesssim 0.08 \max(c_1^i)$ (both allowing for sizeable modifications of $\Delta\gamma$) and $|X_{bb}^{d'}| \lesssim 0.13 \max(c_1^i)$. In fact, while the $Z \rightarrow b\bar{b}$ anomaly cannot be fully resolved in this model, the data prefers non-zero $b-d'$ mixing with $s_{bD} = 0.05(4)$ (assuming negligible d' mixing with first two generations). This is enough to allow for $\mathcal{O}(1)$ modification of y_{bb} and thus $R_{b\bar{b}}$ at order $1/\Lambda$. In particular neglecting also the m_b/M_D suppressed right-handed $b-d'$ mixing one can write

$$y_{bb} \simeq \frac{m_b}{v} + s_{bD} c_1^b \frac{v}{\Lambda} = \frac{m_b}{v} \left(1 + s_{bD} c_1^b \frac{v^2}{m_b \Lambda} \right). \quad (37)$$

On the other hand, $b-d'$ mixing has negligible effects on the modifications to gluon fusion production and Higgs decay to two photons

$$R_{gg} = \frac{0.057^2 + |0.65 + 0.67 y_{d'd'}|^2}{0.65^2}, \quad R_{\gamma\gamma} = \frac{|-6.5 + 0.45 y_{d'd'}|^2}{|-6.5|^2}, \quad (38)$$

where c_2 contributions to $y_{d'd'}$ dominate as $y_{d'd'} = -c_{bD} c_2 v^2 / \Lambda m_{d'}$. The resulting predictions from the non-renormalizable model with a singlet down-type vector-like quark are presented by the red-dotted curves in the $(R_{gg}, R_{\gamma\gamma})$ plane in Fig. 1. Again we have used $|c_2|/\Lambda \leq 1 \text{ TeV}^{-1}$ and $m_{d'} > 350 \text{ GeV}$ as suggested by direct searches (see the related discussion below). Allowing for $R_{bb} \neq 1$ (right plot), the preferred parameter regions for $y_{d'd'}$ at 68% C.L. are $y_{d'd'} = -0.16_{-0.14}^{+0.19}$ (when marginalizing over $\Delta\gamma$) and $y_{d'd'} = -0.17_{-0.13}^{+0.17}$ (when fixing $\Delta\gamma = 0$). Consequently, current Higgs data are not yet very constraining in this context. On the other hand, in absence of significant d' mixing with lighter quarks (for $R_{bb} = 1$ and $\Delta\gamma = 0$ in left plot of Fig. 1), the Higgs data already give an interesting constraint (as discussed below) on $y_{d'd'} = -0.12 \pm 0.08$. Marginalizing instead over $y_{d'd'}$ and R_{bb} in this scenario, we obtain a bound on $\Delta\gamma < 1.2$ at 95% C.L. This implies $|X_{dd'}^{d'} + X_{ss}^{d'}|v/\Lambda < 0.027$. Similarly, marginalizing over $y_{d'd'}$ and $\Delta\gamma$, we get $R_{bb} < 2.3$, implying $|0.019 - X_{bb}^{d'}|v/\Lambda < 0.038$.

Finally, turning to the naturalness condition in (2), for the case of a single vector-like down-type singlet quark it reads in the small $b-d'$ mixing limit

$$\frac{m_t^2 + m_{d'}^2 s_{bD}^2}{v^2} = c_{bD} c_2 \frac{m_{d'}}{\Lambda} + \mathcal{O}(1/\Lambda^2), \quad (39)$$

or equivalently $y_{d'd'} = -s_{bD}^2 - (m_t/m_{d'})^2$ again independent of the cut-off scale Λ . Present Higgs data then provide an indirect constraint on the d' mass, which reads $m_{d'} > 330 \text{ GeV}$ in the zero $b-d'$ mixing case and grows stronger

for non-zero s_{bD} . This is to be compared to direct experimental searches [37], which yield $m_{d'} > 480$ GeV for the renormalizable down-type singlet model dominantly mixing with the b . In this case however, the direct constraint is dominated by the $d' \rightarrow Wt$ decay signature. Enhancing the $d' \rightarrow bh$ rate in the small $b - d'$ mixing limit through the coupling $y_{d'b} \simeq -c_{bD}c'_{bD}c_1^b v/\Lambda$ can thus naturally relax it to $m_{d'} \gtrsim 350$ GeV; dominant (but small) mixing with the first two generations possibly even further. In light of this, the Higgs data already provide a complementary and competitive handle on such models.

V. DOUBLET VECTOR-LIKE QUARK

A. Renormalizable model

As a final example, we consider the SM extended by a vector-like pair (Q_L, Q_R) in the $\mathbf{2}_{1/6}$ electroweak representation. The most general renormalizable Lagrangian now contains the Yukawa and mass terms

$$-\mathcal{L}_Q^{(0)} = y_d^{ij} \bar{q}_L^i H d_R^j + y_u^{ij} \bar{q}_L^i \tilde{H} u_R^j + y_D^i \bar{Q}_L H d_R^i + y_U^i \bar{Q}_L \tilde{H} u_R^i + M_Q \bar{Q}_L Q_R + \text{h.c.} \quad (40)$$

The mass matrices of both up- and down-like quarks after EWSB now have the form

$$\mathcal{M}_u = \begin{pmatrix} y_u v/\sqrt{2} & 0 \\ y_U v/\sqrt{2} & M_Q \end{pmatrix}, \quad \mathcal{M}_d = \begin{pmatrix} y_d v/\sqrt{2} & 0 \\ y_D v/\sqrt{2} & M_Q \end{pmatrix}. \quad (41)$$

In the quark mass eigenbasis the weak gauge and Higgs interactions of 4 (u, c, t, u') physical up-like and 4 (d, s, b, d') down-like quarks are governed by two 4×4 matrices, a unitary V^L and a non-unitary V^R . Consequently $X_{ij}^{u,d} = \delta_{ij}$, while $Y_{ij}^{u,d}$ are hermitian and constrained as

$$|Y^u|_{3 \times 3} < \begin{bmatrix} 0.11 & 2.1 \times 10^{-4} & 0.14 \\ & 0.018 & 0.14 \\ & & - \end{bmatrix}, \quad |Y^d|_{3 \times 3} < \begin{bmatrix} 0.1 & 1.4 \times 10^{-5} & 4 \times 10^{-4} \\ & 0.21 & 0.001 \\ & & 0.03 \end{bmatrix}. \quad (42)$$

Due to such severe experimental bounds on the mixing of vector-like doublet components with the first two quark generations, and also with the b quark, the dominant effect on Higgs phenomenology could possibly come from the mixing in the top sector (via induced Y_{tt}^u), which remains unconstrained at the tree-level. However, as shown in [34] the (right-handed) mixing angles in the top ($t - u'$) and bottom ($b - d'$) quark sectors are related via the mass splitting between the two extra quark states u' and d' as

$$m_{d'}^2 [1 - s_{bD}^2 (1 - r_{bd'}^2)] = m_{u'}^2 [1 - s_{tU}^2 (1 - r_{tu'}^2)], \quad (43)$$

where $r_{ij} \equiv m_i/m_j$. Left-handed and right-handed mixing angles are now related through $\tan \theta'_{ij} = r_{ij'} \tan \theta_{ij}$. At the one-loop level, the $u' - d'$ mass splitting ($\Delta m_Q \equiv m_{u'} - m_{d'}$) is constrained from EW precision measurements. In particular, $Z \rightarrow b\bar{b}$ observables constrain the $b - d'$ and $t - u'$ mixing angles as shown in Fig. 5 (see appendix C for details). Together with a constraint from the ρ parameter, this gives the bound on Δm_Q as shown in Fig. 3 (the narrowest purple bands).⁹ Taking all this into account (in particular discarding the fine-tuned solution for large negative Δm_Q), we find (in accordance with [34]) that the vector-like quark doublet with renormalizable couplings has unobservable effects in single Higgs production and decay processes.

B. Non-renormalizable models

At the non-renormalizable level, the doublet vector-like quark model offers a somewhat richer structure than the singlet examples. Namely, the introduction of dimension five operators allows to shift the vector-like mass independently for both isospin components of Q via the insertion of an iso-triplet combination of Higgs fields

$$M_Q \bar{Q}_R Q_L \rightarrow M_Q \bar{Q}_R Q_L + \frac{c_2^+}{\Lambda} (v^2/2 - |H|^2) \bar{Q}_R Q_L + \frac{c_2^-}{\Lambda} \bar{Q}_R (H H^\dagger - \tilde{H} \tilde{H}^\dagger) Q_L. \quad (44)$$

⁹ Note that we do not find a bound as strong as reported in [34]. The resulting implications for Higgs phenomenology remain however qualitatively unchanged.

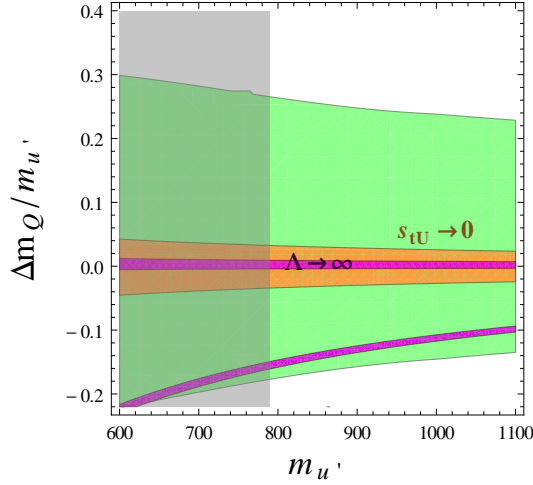


Figure 3: Allowed region at 95% C.L. for $u' - d'$ mass splitting as a function of the u' quark mass in models with a doublet vector-like quark. The narrowest purple bands apply to the renormalizable model, the middle orange band stands for the non-renormalizable model in the zero $t - u'$ mixing limit, while the broadest green band is for the non-renormalizable model with non-zero $t - u'$ mixing effects allowed by $Z \rightarrow b\bar{b}$ data. The gray area marks the ATLAS experimental search bound on the renormalizable model using the $u' \rightarrow th$ decay signature [35].

Similarly, one can now introduce two new operators (via iso-singlet and iso-triplet Higgs field insertions)

$$-\mathcal{L}_Q^{(1)} = \frac{(c_1^+)^i}{\Lambda} (v^2/2 - |H|^2) \bar{Q}_R q_L^i + \frac{(c_1^-)^i}{\Lambda} \bar{Q}_R (HH^\dagger - \tilde{H}\tilde{H}^\dagger) q_L^i. \quad (45)$$

The two isospin breaking corrections (proportional to $c_{1,2}^-$) now necessarily induce corrections to quark masses and mixings. In particular, the resulting changes to $\mathcal{M}_{u,d}$ can be parametrized as

$$(y_{u,d})^{ij} \rightarrow (y'_{u,d})^{ij} \equiv (y_{u,d})^{ij} \frac{\bar{M}_{U,D}}{M_{U,D}} \mp \frac{v^2 (y_{U,D})^i (c_1^-)^j}{2\Lambda M_{U,D}}, \quad (46)$$

$$(y_{U,D})^i \rightarrow (y'_{U,D})^i \equiv (y_{U,D})^i \frac{\bar{M}_{U,D}}{M_{U,D}} \pm \frac{v^2 (y_{u,d})^{ij} (c_1^-)_j}{2\Lambda M_{U,D}}, \quad (47)$$

$$M_Q \rightarrow M_{U,D}, \quad (48)$$

where $M_{U,D} \equiv \sqrt{\bar{M}_{U,D}^2 + v^4 ((c_1^-)^i (c_1^-)_i^*) / 4\Lambda^2}$ and $\bar{M}_{U,D} \equiv M_Q \pm v^2 c_2^- / 2\Lambda$. The only observable effect of these shifts is the breaking of correlation between the masses and mixing angles in the up- and down-type quark sectors, such that $\Delta m_Q \equiv m_{u'} - m_{d'}$ becomes an independent free parameter, given in the zero-mixing limit (when $y'_{U,D} = 0$) solely by $\Delta m_Q = v^2 c_2^- / \Lambda$. At the one-loop level it will affect the ρ parameter as

$$\Delta\rho \simeq -\frac{\alpha N_C}{6\pi s_W^2} \frac{(\Delta m_Q)^2}{m_W^2}, \quad (49)$$

where we have only kept the leading Δm_Q dependence. The resulting constraint is shown in Fig. 3 (in middle orange band). However, if we also include non-zero $t - u'$ mixing effects, marginalizing over the allowed values of s_{tU} from $Z \rightarrow b\bar{b}$ data we obtain a much weaker bound on Δm_Q shown in the uppermost (green) band in Fig. 3. In our numerical evaluation we employ the full one-loop formula for $\Delta\rho$, which can be found in Appendix D. We thus conclude that after including the contributions of leading higher dimensional operators, the isospin components of a TeV scale vector-like quark doublet can be split by as much as 30%. Although this has no observable consequences for Higgs phenomenology, it can have profound implications for direct u' searches if the $u' \rightarrow d'W$ decay channel becomes kinematically allowed.

The new Higgs interactions in the mass eigenbasis are again of the form (8), where now $X^{u,d'} = U_R^{u,d} \cdot [(0,0), (c_1^\pm \pm c_1^\mp, c_2^\pm \pm c_2^\mp)]^* \cdot U_L^{u,d\prime}$ or explicitly $(X^{u,d'})_{ij} = (U_R^{u,d})_{i4} [(c_1^\pm \pm c_1^\mp)^k (U_L^{u,d})_{jk}^* + (c_2^\pm \pm c_2^\mp) (U_L^{u,d})_{j4}^*]$. They are thus constrained indirectly by bounds on $Y^{u,d}$, since now $|(U_R^{u,d})_{i4}|^2 = Y_{ii}^{u,d}$. Taking into account also the relation

$|(U_L^{u,d})_{i4}|^2 = (m_i/M_{U,D})^2 |(U_L^{u,d})_{i4}|^2$, we can safely neglect c_2^\pm contributions and obtain $X_{uu}^{u'} \lesssim 0.35 \max[(c_1^+ + c_1^-)^i]$, $X_{cc}^{u'} \lesssim 0.13 \max[(c_1^+ + c_1^-)^i]$, $X_{dd}^{d'} \lesssim 0.30 \max[(c_1^+ - c_1^-)^i]$, $X_{ss}^{d'} \lesssim 0.40 \max[(c_1^+ - c_1^-)^i]$ and $X_{bb}^{d'} \lesssim 0.11 \max[(c_1^+ - c_1^-)^i]$. Significant effects in $\Delta\gamma$ and R_{bb} are thus possible and can be used to constrain the diagonal entries of $X^{u,d'}$.

Additional interesting effects again appear in loop induced Higgs processes. Higgs decays to pairs of gluons or photons are modified by additional heavy particles in the loop

$$R_{gg} = \frac{|0.68(r_x + r_y) - 0.040|^2 + 0.057^2}{0.65^2}, \quad R_{\gamma\gamma} = \frac{|-8.3 + 1.8r_x + 0.45r_y|^2}{|-6.5|^2}, \quad (50)$$

where to order $1/\Lambda$ and including $t - u'$ mixing

$$\begin{aligned} r_x &\equiv y_{tt} \frac{v}{m_t} + y_{u'u'} \frac{v}{m_{u'}} \\ &= 1 + s_{tU} ((c_1^+ + c_1^-)^t c'_{tU} - (c_2^+ + c_2^-) s'_{tU}) \frac{v^2}{\Lambda m_t} - c_{tU} ((c_1^+ + c_1^-)^t s'_{tU} + (c_2^+ + c_2^-) c'_{tU}) \frac{v^2}{\Lambda m_{u'}}, \end{aligned} \quad (51)$$

and

$$r_y \equiv y_{d'd'} \frac{v}{m_{d'}} = -\frac{v^2}{\Lambda m_{d'}} (c_2^+ - c_2^-). \quad (52)$$

Taking into account the bound on $t - u'$ mixing, a good approximation for $r_x = 1 + s_{tU} \frac{(c_1^+ + c_1^-)^t v^2}{\Lambda m_t} - \frac{(c_2^+ + c_2^-) v^2}{\Lambda m_{u'}}$. There is no correlation between R_{gg} and $R_{\gamma\gamma}$ in general, unless one imposes additional constraints on the parameters.

Therefore, the resulting predictions from the non-renormalizable model with a doublet vector-like quark are given by a region (dashed-black contour) in the $(R_{gg}, R_{\gamma\gamma})$ plane of Fig. 1 left, in the case when modification of $\Delta\gamma$ is allowed and $R_{bb} = 1$, and on Fig. 1 right, when sizable modification of R_{bb} is allowed as well.¹⁰ We have assumed $|c_{1,2}^{\pm}|/\Lambda \leq 1 \text{ TeV}^{-1}$ and $m_{q'} > 790 \text{ GeV}$ as suggested by direct searches [35]. Also, we take the $t - u'$ mixing angle to be within the 95% C.L. experimental bound discussed above ($s_{tU} \lesssim 0.35$).

For small mixing and negligible isospin breaking, masses of u' and d' quarks are degenerate and $r_y = r_x - 1 = -\frac{v^2}{\Lambda m_{q'}} c_2^+$. Allowing for modification of $\Delta\gamma$ and fixing $R_{bb} = 1$, the resulting predictions in this scenario are presented by the green-dashed curve in the $(R_{gg}, R_{\gamma\gamma})$ plane in Fig. 1 left. Allowing for sizable modification of R_{bb} as well, the predictions are presented by the green-dashed curve in the $(R_{gg}, R_{\gamma\gamma})$ plane in Fig. 1 right. Again we have assumed $|c_2^+|/\Lambda \leq 1 \text{ TeV}^{-1}$ and $m_{q'} > 790 \text{ GeV}$. In particular, the preferred parameter regions for r_y at 68% C.L. are $r_y = -0.09_{-0.06}^{+0.09}$ (marginalizing over both R_{bb} and $\Delta\gamma$), $r_y = -0.09_{-0.06}^{+0.08}$ (marginalising over R_{bb} but fixing $\Delta\gamma$), $r_y = -0.07_{-0.04}^{+0.09}$ (fixing $R_{bb} = 1$ and marginalizing over $\Delta\gamma$) and finally $r_y = -0.06 \pm 0.04$ (fixing both R_{bb} and $\Delta\gamma$ to their SM values).

Also in the unmixed isospin symmetric doublet scenario we can get $\Delta\gamma < 1.0$ at 95% C.L. after marginalizing over r_y and R_{bb} . This implies $|X_{uu}^{u'} + X_{cc}^{u'} + X_{dd}^{d'} + X_{ss}^{d'}|v/\Lambda < 0.025$. Conversely, marginalizing over r_y and $\Delta\gamma$, we get $R_{bb} < 2.1$ implying $|0.019 - X_{bb}^{d'}v/\Lambda| < 0.036$. We have checked that these results remain stable even in presence of small $t - u'$ mixing and isospin breaking.

In this scenario, the Higgs mass naturalness condition reads

$$\frac{m_t^2}{v^2} = 2c_2^+ \frac{m_{q'}}{\Lambda} + \mathcal{O}(1/\Lambda^2), \quad (53)$$

or equivalently $r_y = -(m_t/\sqrt{2}m_{q'})^2$. This condition allows to put an indirect bound on the mass of q' to be 390 GeV at 95% C.L. in the case of fixed R_{bb} .

Turning to direct searches, the most severe bound on u' in the renormalizable model with a doublet vector-like quark assuming dominant but small mixing with the third generation, $m_{u'} > 790 \text{ GeV}$ [35] is given by the ATLAS experimental search using the $u' \rightarrow th$ decay signature. In the non-renormalizable model the relevant couplings are given by $y_{tu'} = s_{tU} c_{tU} m_{u'}/v + s_{tU} (s'_{tU} (c_1^+ + c_1^-)^t + c'_{tU} (c_2^+ + c_2^-))v/\Lambda$ and $y_{u't} = s_{tU} c_{tU} m_t/v - c_{tU} (c'_{tU} (c_1^+ + c_1^-)^t - s'_{tU} (c_2^+ + c_2^-))v/\Lambda$. It is then easy to check that again compared to $u' \rightarrow tZ$ and $u' \rightarrow bW$ rates, the $1/\Lambda$ corrections can in principle enhance $\mathcal{B}(u' \rightarrow th)$ in the small s_{tU} limit but cannot reduce it significantly below its

¹⁰ As in the case of the non-renormalizable model with a down-like vector-like quark, y_{bb} can receive $\mathcal{O}(1)$ modifications even for small $b - d'$ mixing.

| Coupling | Constraint | Reference |
|--------------------------------|-------------------------|------------|
| $ X_{cu}^u , Y_{cu}^u $ | $< 2.1 \times 10^{-4}$ | [12, 13] |
| $ X_{tu,tc}^u , Y_{tu,tc}^u $ | < 0.14 | Appendix A |
| $ X_{ds}^d , Y_{ds}^d $ | $< 1.4 \times 10^{-5}$ | Appendix B |
| $ X_{db}^d , Y_{db}^d $ | $< 4 \times 10^{-4}$ | |
| $ X_{sb}^d , Y_{sb}^d $ | $< 1 \times 10^{-3}$ | |
| δX_{uu}^u | $-0.0001(6)$ | [9] |
| δX_{cc}^u | $-0.0020(13)$ | Appendix C |
| δX_{dd}^d | $-0.0031(20)$ | Appendix C |
| δX_{ss}^d | $-0.002(3)$ | |
| δX_{bb}^d | $0.0027(15)$ | |
| δY_{uu}^u | $0.035(40)$ | Appendix C |
| δY_{cc}^u | $-0.003(9)$ | |
| δY_{dd}^d | $0.030(35)$ | |
| δY_{ss}^d | $-0.05^{+0.08}_{-0.06}$ | |
| δY_{bb}^d | $-0.018(6)$ | |

Table II: Compilation of phenomenological constraints on Higgs (and Z) couplings to SM quarks in renormalizable vector-like quark models (see Eqs. (6), (7)) from precision flavor and electroweak observables. All upper bounds are given at 95% C.L. For discussion of δX_{tt}^u , δY_{tt}^u constraints see Sections III A and V A, respectively.

value in the renormalizable model. However, the significant $u' - d'$ mass splitting allowed by present data when including dimension five contributions, reopens the possibility that the dominant decay channel of u' is actually $u' \rightarrow d'W$, in which case the existing direct search constraints are considerably relaxed and dominated by searches for the lighter isospin component via $d' \rightarrow tW$ and $d' \rightarrow bh$ decay signatures (in the case of dominant mixing with the third generation). Consequently, in such scenarios $u'(d')$ masses as low as $m_{u'(d')} \gtrsim 400$ GeV (300 GeV) could still be viable.

VI. CONCLUSIONS

We have systematically investigated the impact of dynamical vector-like quarks, accommodated within SM gauge representations and charges, on Higgs physics. In particular, we have considered the weak singlet up-type, singlet down-type and doublet vector-like quarks, potentially mixing with all three known generations of chiral quarks, and have updated the most relevant constraints on such scenarios from low energy flavour phenomenology and electroweak precision measurements. The resulting general constraints on the renormalizable and leading non-renormalizable quark-Higgs interactions are summarised in Tables II and III, respectively.

Within the renormalizable SM extended by additional vector-like quarks, we have shown generally that Higgs couplings to the known three generations of quarks need to remain SM-like regardless of the extra quark masses. This feature is a consequence of the fact that precision flavour and electro-weak observables are affected by the mixing of vector-like and chiral quarks, some of them already at the tree level. Consequently, Higgs decay widths to light quark pairs, gg and $\gamma\gamma$ cannot deviate significantly from their SM predictions.

A singular feature of models with vector-like fermions is that non-renormalizable contributions sensitive to physics at the cut-off scale of the effective low energy theory appear already at dimension five. The inclusion of such higher-dimensional operators is essential in models that aim to cancel dominant quadratic divergences to the Higgs boson mass coming from top quark loops with new fermionic contributions. Contrary to the renormalizable models (see however [39]), they also predict interesting effects in Higgs phenomenology. We have investigated such contributions for all three types of additional vector-like quarks mixing with SM generations (see Fig. 1). The most important consequences for Higgs physics are possible significant enhancements in Higgs decay rates to pairs of light ($u\bar{u}$, $d\bar{d}$, $s\bar{s}$, $c\bar{c}$) quarks, which may still account for a significant fraction of the total Higgs decay width. This is possible due to a simultaneous strong modification of the Higgs production by gluon fusion $gg \rightarrow h$ (up to 50% deviation from SM predictions, while the $h \rightarrow \gamma\gamma$ decay width can receive modifications up to 10%). Such a possibility could thus be tested by future more accurate determinations of vector boson fusion and (W , Z or $t\bar{t}$) associated Higgs production. In addition, a possible modification of the Higgs coupling to b quarks in models containing down-type vector-like quarks

| Coupling | Constraint | Reference |
|---|----------------------|---------------|
| $ X_{uc,cu}^{u'} v/\Lambda$ | $< 7 \times 10^{-5}$ | [16] |
| $\sqrt{ X_{tu,tc}^{u'} ^2 + X_{ut,ct}^{u'} ^2}v/\Lambda$ | < 0.34 | |
| $ X_{sd,ds}^{d'} v/\Lambda$ | $< 2 \times 10^{-5}$ | |
| $ X_{bd,db}^{d'} v/\Lambda$ | $< 2 \times 10^{-4}$ | |
| $ X_{sb,bs}^{d'} v/\Lambda$ | $< 1 \times 10^{-3}$ | |
| $\sqrt{ X_{uu}^{u'} ^2 + X_{cc}^{u'} ^2}v/\Lambda$ | < 0.022 | Section III B |
| $\sqrt{ X_{dd}^{d'} ^2 + X_{ss}^{d'} ^2}v/\Lambda$ | < 0.027 | Section IV B |
| $\sqrt{ X_{uu}^{u'} ^2 + X_{cc}^{u'} ^2 + X_{dd}^{d'} ^2 + X_{ss}^{d'} ^2}v/\Lambda$ | < 0.025 | Section V B |
| $ 0.019 - X_{bb}^{d'}v/\Lambda $ | < 0.038 | Section IV B |
| | < 0.036 | Section V B |

Table III: Compilation of constraints on additional Higgs couplings to SM quarks due to dimension five operators in models with vector-like quarks (see Eq. (8)). The off-diagonal couplings are bounded by low energy flavor observables, whereas upper limits on the diagonal ones were estimated from the fit to current Higgs data. All bounds are given at 95% C.L. For discussion of $\delta X_{tt}^{u'}$ constraints within up-type singlet and doublet vector-like quark scenarios see Sections III B and V B, respectively.

will be probed by future precise measurements of the $h \rightarrow b\bar{b}$ decay.¹¹

Interestingly, current Higgs data are perfectly consistent with (and even exhibit a slight preference for) the possibility that vector-like quarks contribute to the cancellation of the top loop quadratic divergence to the Higgs mass. Conversely in some cases, a fit to existing Higgs measurements under such an assumption already offers competitive and robust constraints on vector-like quark masses in comparison with results of direct experimental searches which need to rely on particular decay signatures. In the example of a weak doublet of vector-like quarks, we have shown that dimension five contributions allow to relax the stringent bounds on the mass splitting between the two isospin states. Consequently the decay of the heavier doublet component to the lighter one with the emission of a W boson may become kinematically allowed, affecting the relevant experimental signatures. More generally in presence of dimension five contributions, vector-like quark decay widths are naturally dominated by decay channels involving the Higgs. Future dedicated experimental searches for such particular signatures (as exemplified in [35], see also [40]) could thus shed light on the relevance of vector-like quarks in the solution to the SM hierarchy problem.

Acknowledgments

This work was supported in part by the Slovenian research agency and the Ad futura Programme of the Slovenian Human Resources and Scholarship Fund.

Appendix A: CKM non-unitarity and Z mediated FCNCs in top quark production and decays

In absence of right-handed charged currents, experimental constraints on $\sum_{i=d,s,b} |V_{ti}^L|^2 = 1 - \Delta_t^u \leq 1$ and also $|V_{tb}^L|^2$ can be obtained from the measurements of the (t -channel) single top production cross-section (σ_t) at the LHC and the fraction of top decays to Wb pairs in $t\bar{t}$ production (R). Assuming $t \rightarrow Wq$ channels dominate the top decay width, to a very good approximation R is given by $R \simeq |V_{tb}^L|^2 / (\sum_{i=d,s,b} |V_{ti}^L|^2)$ and we can use the recent CMS result $R^{\text{exp}} = 0.98 \pm 0.04$ [41]. Note that this measurement alone requires that $|V_{tb}^L| \gg |V_{ts}^L|, |V_{td}^L|$. The relevant t -channel single top production cross-section can then be written as $\sigma_t \simeq \sigma_t^{\text{SM}} |V_{tb}^L|^2 R$, where the SM prediction of $\sigma_t^{\text{SM}} = 64.6_{-2.0}^{+2.7}$ pb [42] is obtained with $|V_{tb}^L| = 1$ and $R = 1$. We compare this to the weighted average of the recent ATLAS [43], and CMS [44] results ($\sigma_t^{\text{exp}} = 68.5 \pm 5.8$ pb). Performing a χ^2 fit of the two experimental quantities in terms of $|V_{tb}^L|^2$ and $\sum_{i=d,s,b} |V_{ti}^L|^2$ (and taking into account theoretical constraints $\sum_{i=d,s,b} |V_{ti}^L|^2 \leq 1$ and $|V_{ti}^L| > 0$)

¹¹ A direct determination of Higgs decays to charmed and light jets would also be enlightening in this respect.

we obtain the 95% C.L. lower bounds of

$$|V_{tb}^L|^2 > 0.85, \quad \sum_{i=d,s,b} |V_{ti}^L|^2 > 0.87. \quad (\text{A1})$$

In models with up-type weak singlet vector-like quarks, $|X_{ut}|$ and $|X_{ct}|$ will contribute to FCNC top decays. Combined with σ_t and R , the experimental bounds on $\mathcal{B}(t \rightarrow Zq)$ can then be used to constrain $\sqrt{|X_{ut}|^2 + |X_{ct}|^2} \equiv |X_{tu,tc}|$. The presence of these new decay channels in principle also needs to be accommodated in σ_t and R by writing

$$\sigma_t = \sigma_{\text{SM}} |V_{tb}^L|^2 \left(\frac{1}{R} + \rho_{WZ} \frac{|X_{tu,tc}|^2}{|V_{tb}^L|^2} \right)^{-1}, \quad (\text{A2})$$

where

$$\rho_{WZ} = \frac{1}{2} \frac{(2M_Z^2 + m_t^2) \left(1 - \frac{M_Z^2}{m_t^2}\right)^2}{(2M_W^2 + m_t^2) \left(1 - \frac{M_W^2}{m_t^2}\right)^2}, \quad (\text{A3})$$

takes into account the dominant phase-space difference in $t \rightarrow Wq$ and $t \rightarrow Zq$ decays. In addition, searches for $t \rightarrow Zq$ typically assume $\mathcal{B}(t \rightarrow Wb) + \mathcal{B}(t \rightarrow Zq) = 1$ and $|V_{tb}^L| = 1$. In presence of $|V_{tb}^L| < 1$, the experimental results should instead be compared to

$$\bar{\mathcal{B}}(t \rightarrow Zq) = \left(1 + \frac{|V_{tb}^L|^2}{\rho |X_{tu,tc}|^2} \right)^{-1}. \quad (\text{A4})$$

Including the recent ATLAS result $\mathcal{B}(t \rightarrow Zq)^{\text{exp}} < 0.73\%$ [45] in our fit, we first observe that the presence of FCNCs has no observable effect on the results in eq. (A2). On the other hand, we can obtain an upper bound on $|X_{tu,tc}| < 0.14$ at 95% C.L..

Although the presence of right-handed charged currents complicates the analysis of top production and decays, a robust bound on $|Y_{tu,tc}|$ and also $|V_{tb}^R|$ can nonetheless be obtained. To a good approximation namely in this case

$$R = \frac{|V_{tb}^L|^2 + |V_{tb}^R|^2}{\sum_{i=d,s,b} (|V_{ti}^L|^2 + |V_{ti}^R|^2)}, \quad (\text{A5})$$

and thus experimentally $|V_{tb}^L|^2 + |V_{tb}^R|^2 \gg |V_{ts}^L|^2, |V_{ts}^R|^2, |V_{td}^L|^2, |V_{td}^R|^2$. In addition, the presence of V_{tb}^R will affect single top production as

$$\sigma_t = \sigma_{\text{SM}} (|V_{tb}^L|^2 + \kappa_R |V_{tb}^R|^2) \left(\frac{1}{R} + \rho_{WZ} \frac{|Y_{tu,tc}|^2}{|V_{tb}^L|^2 + |V_{tb}^R|^2} \right)^{-1}, \quad (\text{A6})$$

where $\kappa_R \simeq 0.92$ [46]. Finally, V_{tb}^R contributes to the positive W helicity fraction (\mathcal{F}_+) in top decays as

$$\mathcal{F}_+ = \frac{|V_{tb}^L|^2}{|V_{tb}^L|^2 + |V_{tb}^R|^2} \mathcal{F}_+^{\text{SM}} + \eta_+^R \frac{|V_{tb}^R|^2}{|V_{tb}^L|^2 + |V_{tb}^R|^2} \frac{2x}{(1+2x)}, \quad (\text{A7})$$

where $\mathcal{F}_+^{\text{SM}} = 0.0017(1)$ [47], $x = (m_W/m_t)^2$ and $\eta_+^R = 0.93$ parametrizes NLO QCD corrections [48]. Using the recent determination of $\mathcal{F}_+^{\text{exp}} = 0.01(5)$ by ATLAS [49] we obtain $|V_{tb}^R| < 0.2|V_{tb}^L|$. Thus we may conservatively use the results of the previous paragraphs also to constrain $|V_{tb}^L| > 0.85$ and $|Y_{tu,tc}| < 0.14$.

Appendix B: Bounds on down-type quark mixing with vector-like weak singlets and doublets from rare K and B_q processes

Model independent bounds on the off-diagonal entries of X^d, Y^d in models with additional vector-like down-type weak singlet and weak doublet quarks respectively can be obtained from their tree-level (Z -mediated) contributions to FCNCs involving down-type quarks. For example, a bound on X_{ds}^d, Y_{ds}^d can be extracted from the $K_L \rightarrow \mu^+ \mu^-$ decay. We use a conservative estimate for the pure short distance branching fraction $\mathcal{B}(K_L \rightarrow \mu^+ \mu^-)_{SD}^{\text{exp}} < 2.5 \times 10^{-9}$,

obtained using dispersive techniques [50], as a 1σ upper bound. Neglecting the much smaller SM contributions, the X_{ds}^d contribution can be written as

$$\mathcal{B}(K_L \rightarrow \mu^+ \mu^-)^X = \frac{G_F^2}{16\pi} f_K^2 m_K \tau_{K_L} m_\mu^2 \sqrt{1 - \frac{4m_\mu^2}{m_K^2}} \text{Re}(X_{sd})^2. \quad (\text{B1})$$

Using the inputs for G_F , masses and lifetimes from [10] and also $f_K = 155.37(34)$ MeV [9] we obtain $\text{Re}(X_{sd}) < 1 \times 10^{-5}$ (the same result applies also to Y_{sd}). Since much stricter bounds are expected on $\text{Im}(X_{sd})$ ($\text{Im}(Y_{sd})$) from the precise knowledge of ϵ_K , we interpret the above values as conservative constraints also on the moduli of X_{sd} and Y_{sd} .

In the B_d sector, X_{bd} contributes at the tree-level both to $B_d \rightarrow \mu^+ \mu^-$, as well as in $B^0 - \bar{B}^0$ mixing. Neglecting X_{bd} loop level corrections due to CKM non-unitarity and dynamical vector-like quarks running in the loop, the $B_d \rightarrow \mu^+ \mu^-$ branching fraction can be written as

$$\mathcal{B}(B_d \rightarrow \mu^+ \mu^-) = \frac{G_F^2}{8\pi} f_{B_d}^2 m_{B_d} \tau_{B_d} m_\mu^2 \sqrt{1 - \frac{4m_\mu^2}{m_{B_d}^2}} \left| \lambda_{bd}^t C_{dB=1}^{\text{SM}} + \frac{X_{bd}}{\sqrt{2}} \right|^2, \quad (\text{B2})$$

with $\lambda_{bd}^t = V_{td}^L V_{tb}^{L*}$ the relevant CKM combination and the SM Wilson coefficient given by

$$C_{dB=1}^{\text{SM}} = \frac{\alpha}{\sqrt{2}\pi s_W^2} \eta_Y Y_0 \left(\frac{\bar{m}_t^2}{m_W^2} \right). \quad (\text{B3})$$

Here Y_0 is the relevant Inami-Lim loop function [51]

$$Y_0(x) = \frac{x}{8} \left[\frac{4-x}{1-x} + \frac{3x}{(1-x)^2} \ln x \right], \quad (\text{B4})$$

while $\eta_Y = 1.01$ [52] parametrizes higher order QCD corrections. For the values of SM input parameters (in particular α_{em} , s_W and \bar{m}_t) we follow the prescription of [52], and we use $f_B = 190.6 \pm 4.7$ [53]. In the $B^0 - \bar{B}^0$ system, the two most relevant observables are the mass-difference between the two B_d mass eigenstates (Δm_d) and the CP violating phase in the mixing (β_d). Since the corresponding width difference ($\Delta\Gamma_d$) is small $|\Delta\Gamma_d| \ll |\Delta m_d|$, one can write

$$\Delta m_d \simeq 2|M_{12}^d|, \quad \sin 2\beta_d = \frac{\text{Im}(M_{12}^d)}{|M_{12}^d|}, \quad \text{where} \quad M_{12}^d = \frac{G_F}{12} m_{B_d} f_{B_d}^2 B_{B_d} \left(\lambda_{bd}^t{}^2 C_{dB=2}^{\text{SM}} + \frac{X_{bd}^2}{\sqrt{2}} \right). \quad (\text{B5})$$

with the SM Wilson coefficient given by

$$C_{dB=2}^{\text{SM}} = \frac{\alpha}{\sqrt{2}\pi s_W^2} \eta_B S \left(\frac{\bar{m}_t^2}{m_W^2} \right). \quad (\text{B6})$$

Here again S is the relevant Inami-Lim loop function [51]

$$S(x) = \frac{x}{2} \left[\frac{1}{2} + \frac{3}{2} \frac{1-3x}{(1-x)^2} - \frac{3x^2}{(1-x)^3} \ln x \right], \quad (\text{B7})$$

while $\eta_B = 0.939$ [55] parametrizes higher order QCD corrections. In addition we use $f_{B_d}^2 B_{B_d} = 0.0411 \pm 0.0075$ [54].

In absence of CKM unitarity, we need to determine not only X_{bd} but also the CKM combination λ_{bd}^t . For this purpose we use the radiative rate $B \rightarrow X_d \gamma$, which is unaffected by X_{bd} at the tree-level. Although it receives non-standard contributions proportional to X_{bd} due to CKM non-unitarity and extra down-type quarks in the loops, these are parametrically (loop) suppressed compared to tree-level effects in $B_d \rightarrow \mu^+ \mu^-$ and $B^0 - \bar{B}^0$ mixing. Using the SM recent evaluation [56]

$$\mathcal{B}(B \rightarrow X_d \gamma)_{E_\gamma > 1.6 \text{ GeV}}^{\text{SM}} = \left| \frac{\lambda_{bd}^t}{0.0084} \right|^2 1.54(26) \times 10^{-5}, \quad (\text{B8})$$

and comparing it to the experimental result $\mathcal{B}(B \rightarrow X_d \gamma)_{E_\gamma > 1.6 \text{ GeV}}^{\text{exp}} = 1.41(57) \times 10^{-5}$ [57] we extract $|\lambda_{bd}^t| = 8.0_{-2.0}^{+1.6} \times 10^{-3}$. Plugging this into eq. (B2) we observe that compared to the experimental 95% C.L. upper limit of $\mathcal{B}(B_d \rightarrow \mu^+ \mu^-)^{\text{exp}} < 9.4 \times 10^{-10}$ [58] the λ_{bd}^t contribution can be safely neglected and we obtain a bound on $|X_{bd}| < 4 \times 10^{-4}$. Note that the measurements of $\Delta m_d^{\text{exp}} = 0.507(4)$ ps $^{-1}$ and $\sin 2\beta^{\text{exp}} = 0.679(20)$ [13] cannot be

used to impose a stricter constraint since the phases of λ_{bd}^t and X_{bd} can always be arranged such that cancellations between these contributions weaken the prospective bounds above the one by $\mathcal{B}(B_d \rightarrow \mu^+\mu^-)^{\text{exp}}$.

Finally in the B_s sector we can proceed similarly, with obvious replacements $\lambda_{bd}^t \rightarrow \lambda_{bs}^t$ and $B_d \rightarrow B_s$. We again employ $B \rightarrow X_s \gamma$ to extract $|\lambda_{bs}^t|$ (modulo loop-suppressed X_{bs} effects) as $|\lambda_{bs}^t| = 0.043(2)$ [10] and use $f_{B_s} = 227.6 \pm 5.0$ [53], $f_{B_s}^2 B_{B_s} = 0.0559(68)$ [54] for hadronic inputs. By comparing to the experimental values of $\Delta m_s^{\text{exp}} = 17.719(43) \text{ ps}^{-1}$, $2\beta_s^{\text{exp}} = -0.1(6.1)^\circ$ [13] and $\mathcal{B}(B_s \rightarrow \mu^+\mu^-)^{\text{exp}} = (3.2_{-1.2}^{+1.5}) \times 10^{-9}$ [58] we thus obtain a bound on $|X_{bs}| < 1 \times 10^{-3}$, which is again dominated by the muonic B_s decay rate.

The presence of vector-like weak doublet quarks induces right handed charged and neutral currents among SM quarks. The resulting flavor phenomenology is very rich and deserves a dedicated study. For our purpose however, it suffices to show that to a first approximation, one can actually neglect all terms coming from right handed charged current operators as well as the ones containing extra u', d' quarks in the loops contributing to quark FCNCs. This requires some knowledge of the mixing matrices, which can be expressed through the parameters of the Yukawa sector in terms of an expansion in ratios of mass parameters, which enables us to connect the left and right handed mixing matrices. However, the approximation only holds if such an expansion is justified, as we will check a posteriori. First recall that the up- and down-like quark mass matrices in presence of a single vector-like quark doublet can be written in the form (41). Diagonalizing the products $\mathcal{M}\mathcal{M}^\dagger$ and $\mathcal{M}^\dagger\mathcal{M}$ one obtains the left and right mixing matrices, respectively, which we write in the form (c.f. [59])

$$U_{L,R}^{u,d} = \begin{pmatrix} K_{L,R}^{u,d} & R_{L,R}^{u,d} \\ S_{L,R}^{u,d} & T_{L,R}^{u,d} \end{pmatrix}. \quad (\text{B9})$$

The mixing matrices between the vector-like and chiral quarks can most easily be obtained by starting from a basis of right handed chiral quarks, where $y_{u,d} y_{u,d}^\dagger v^2/2$ are both diagonal, which can be done as the right handed chiral quarks are isosinglets. The mixing $y_{U,D} v/\sqrt{2}$ is bounded by the EW scale v , whereas the Dirac mass m_Q is experimentally required to be larger. Taking thus v/M_Q as the expansion parameter, it can be shown that, to first order in this expansion, both 4×4 right-handed rotation matrices schematically take the form

$$U_R^{u,d} = \begin{pmatrix} \mathbf{1}_{3 \times 3} & \frac{y_{U,D}^\dagger v}{\sqrt{2}M_Q} \\ -\frac{y_{U,D} v}{\sqrt{2}M_Q} & 1 \end{pmatrix} + \mathcal{O}\left(\frac{v^2}{M_Q^2}\right), \quad (\text{B10})$$

so the right handed charged currents are suppressed with $V_{ll}^R \sim \mathcal{O}(v^2/M_Q^2)$ and $V_{lh}^R \sim \mathcal{O}(v/M_Q)$, where l, h stand for light three generations and the extra heavy quarks, respectively.

Turning to the left handed sector, we can choose e.g. a basis of left handed quarks where y_u is diagonal and real and use a unitary transformation to diagonalize y_d . Then we proceed in a similar way as before, and we obtain that, to first nonvanishing order in v/M_Q , $K_L^{u,d}$ from (B9) equal those matrices (no corrections to unity or unitarity). Combining the up and down rotations, the 3×3 upper left submatrix of V^L takes the form

$$V_{ij}^L = (K_L^u)_{ik} (K_L^d)_{jk}^* + (R_L^u)_i (R_L^d)_j^*, \quad i, j, k = 1, 2, 3. \quad (\text{B11})$$

In order to obtain the matrix elements, one has to solve the equations $\mathcal{M}^{u,d} \mathcal{M}^{u,d\dagger} U_L^{u,d} = U_L^{u,d} D_{u,d}^2$, where $D_q = \text{diag}(m_q, m_{q'})$ are the diagonal mass matrices. In the process we require that the entries in $U_L^{u,d}$ mixing chiral and vector-like components ($R_L^{u,d}$ and $S_L^{u,d}$) are smaller than the remaining ones ($K_L^{u,d}$ and $T_L^{u,d}$) in terms of v/M_Q scaling (similar to the case of $U_R^{u,d}$). Also, we assume that the corrections to the masses are small enough so that $m_q, m_{q'}$ are of order v and M_Q , respectively. Consequently the equations for $R_L^{u,d}$ read

$$v^2 (y_{u,d} y_{u,d}^\dagger R_L^{u,d} + y_{u,d} y_{U,D}^\dagger T_L^{u,d}) = 2m_{u',d'}^2 R_L^{u,d}. \quad (\text{B12})$$

With the mentioned assumptions, one can neglect the first term in the above equation, obtaining $R_L^{u,d} = v^2 y_{u,d} y_{U,D}^\dagger / 2m_{u',d'}^2$. Thus, $R_L^{u,d}$ are one order higher than $R_R^{u,d}$ (see B10), the off-diagonal elements in the fourth row and column are of higher order as well, which makes K_L^d a unitary 3×3 matrix to second order in v/M_Q . Consequently all right handed contributions, as well as corrections in the left handed sector are doubly suppressed in the loops of $B_s \rightarrow \mu^+\mu^-$ and we can deduce a conservative bound on the FCNC's by neglecting the afore mentioned corrections, as we have done it in the vector-like singlet quark case. In fact, with the approximations made, the upper bound on $|Y_{bs}|$ is the same as the one on $|X_{bs}|$ in the down-type singlet case.

| Observable | Measured value | SM prediction | Reference |
|---------------------------|----------------|---------------|-----------|
| R_b | 0.21629(66) | 0.21474(3) | [63, 64] |
| A_b | 0.923(20) | 0.9347(1) | [10, 63] |
| A_{FB}^b | 0.0992(16) | 0.1032(6) | [63, 64] |
| $\sigma_{had}[\text{nb}]$ | 41.541(37) | 41.477(9) | [10, 63] |
| $\Gamma_Z[\text{MeV}]$ | 2495.2(2.3) | 2495.5(1.0) | [10, 63] |
| R_c | 0.1721(30) | 0.17227(4) | [10, 63] |
| A_c | 0.670(27) | 0.6680(4) | [10, 63] |
| A_{FB}^c | 0.0707(35) | 0.0739(5) | [10, 63] |

Table IV: Z pole observables used in the analysis and their SM predictions. Correlations between observables are neglected.

Appendix C: Constraining $Z \rightarrow q\bar{q}$

The appearance of Z-mediated FCNC's is generically connected to modifications of diagonal $Zf\bar{f}$ couplings. In the quark sector, such effects can be probed by direct measurements of the hadronic Z decay width, its heavy flavor decays, such as $Z \rightarrow b\bar{b}$, but also at low energies by e.g. atomic parity violation (APV) measurements. In general we can parametrize the chiral $Zq\bar{q}$ couplings in terms of G_M^q ($M = L, R$) as the coefficients multiplying $-\frac{g}{\cos\theta_W}(\bar{q}_M\gamma^\mu q_M)Z_\mu$ and $\delta G_M^q = G_M^q - (G_M^q)_{SM}$ where $(G_M^q)_{SM}$ are given in ref. [60]. In our scenarios $\delta G_L^q = \delta X_{qq}^u/2$ or $\delta G_L^q = -\delta X_{qq}^d/2$, and $\delta G_R^q = Y_{qq}^u/2$ or $\delta G_R^q = -Y_{qq}^d/2$.

Stringent constraints on X_{uu}^u and X_{dd}^d can be derived from APV measurements in ^{133}Cs . The tree level modification of the Z boson couplings to first generation quarks will modify the nuclear weak charge as [61]

$$\delta Q_W(Z, N) = 2(2Z + N)(\delta G_L^u + \delta G_R^u) + 2(Z + 2N)(\delta G_L^d + \delta G_R^d), \quad (\text{C1})$$

where the measured value deviates from the SM expectation by 1.5σ [62]

$$Q_W - Q_W^{SM} \equiv \delta Q_W = 0.65(43). \quad (\text{C2})$$

For the singlet up-like vector-like quark, this constrains $\delta X_{uu}^u = 0.0035(23)$, while for the singlet down-like vector-like quark $\delta X_{dd}^d = -0.0031(20)$. In the doublet case, one has two independent variables δG_R^u and δG_R^d at the tree level, and only a certain linear combination can be constrained, namely $Y_{uu}^u - 1.12Y_{dd}^d = 0.0035(23)$.

Additional constraints can be derived from direct $Z \rightarrow q\bar{q}$ measurements presented in Table IV. In particular, the total Z decay width is given by

$$\Gamma_Z = \Gamma_{\text{inv}} + \Gamma_{\text{lep}} + \Gamma_{\text{had}}. \quad (\text{C3})$$

It incorporates the decays to leptons, where $\Gamma_{\text{lep}} = 251.7$ MeV in the SM, decays into invisible particles (neutrinos), being $\Gamma_{\text{inv}} = 501.6$ MeV in the SM, and the decays into hadrons. The hadronic width is the sum over the decays into all kinematically accessible quarks, that is all SM quarks but the top, $\Gamma_{\text{had}} = \sum_q \Gamma_q$. The partial Z-decay width to light quarks is given by

$$\Gamma_q \equiv \Gamma(Z \rightarrow q\bar{q}) = N_C \frac{G_F M_Z^3}{6\sqrt{2}\pi} \left(R_V^q |G_L^q + G_R^q|^2 + R_A^q |G_L^q - G_R^q|^2 \right) + \Delta_{EW, QCD}^q,$$

with radiator factors R_V^q and R_A^q and non-factorizable radiative correction parameters $\Delta_{EW, QCD}^q$ given in [60]. The fractions of hadronic Z decays involving b quark pairs and c quark pairs are defined as

$$R_b = \frac{\Gamma_b}{\Gamma_{\text{had}}}, \quad R_c = \frac{\Gamma_c}{\Gamma_{\text{had}}}, \quad (\text{C4})$$

respectively. The associated bottom and charm quark left-right asymmetries (A_b and A_c), and forward-backward asymmetries (A_{FB}^b and A_{FB}^c) can be written as

$$A_f = \frac{2\sqrt{1-4z_f} \frac{G_L^f + G_R^f}{G_L^f - G_R^f}}{1 - 4z_f + (1 + 2z_f) \left(\frac{G_L^f + G_R^f}{G_L^f - G_R^f} \right)^2}, \quad A_{FB}^f = \frac{3}{4} A_e A_f, \quad (\text{C5})$$

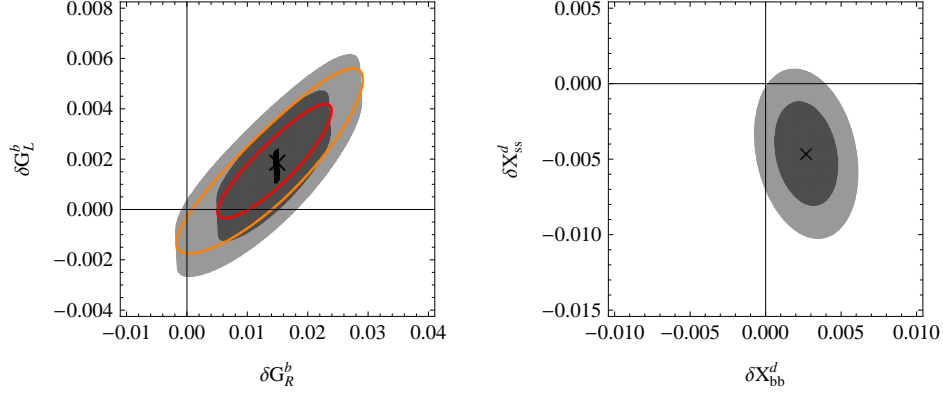


Figure 4: **Left:** Fit of Z-pole data taking $\delta G_{L,R}^q$ for $q = u, d, c, s, b$ as fitting parameters. Best fit point (cross), 1σ (dark gray) and 2σ (light gray) regions are shown in the $(\delta G_R^b, \delta G_L^b)$ plane after marginalizing over the other parameters. The results of the fit for fixed $\delta G_{L,R}^{u,d,c,s} = 0$ are given by the red contour (1σ region) and the orange contour (2σ region). **Right:** The fit of Z-pole data in the model with a singlet down-like vector-like quark. Best fit point (cross), 1σ (dark gray) and 2σ (light gray) regions are shown in $(\delta X_{bb}^d, \delta X_{ss}^d)$ plane.

where $f = b, c$ and $z_f = m_f^2(m_Z)/m_Z^2$. The electron asymmetry parameter is fixed to its SM value, $(A_e)_{SM} = 0.1464$.

Another interesting quantity is the hadronic e^+e^- cross section at the Z pole (σ_{had}). It can be written as

$$\sigma_{had} = \frac{12\pi}{M_Z^2} \frac{\Gamma_e \Gamma_{had}}{\Gamma_Z^2}, \quad (C6)$$

where $\Gamma_e = 84.005$ MeV and $M_Z = 91.1876$ GeV. We perform a χ^2 fit of the data presented in Table IV in terms of δG_M^q as fitting parameters. The results are presented in the $(\delta G_R^b, \delta G_L^b)$ plane, after marginalizing over all other variables, in Fig. 4 left. At the best fit point $\chi_{min}^2 = 3.7$, and the most important observables in the fit are R_b , A_{FB}^b and σ_{had} , which contribute to $\chi_{SM}^2 - \chi_{min}^2$ by 5.6, 4.9 and 1.3, respectively. In the SM reference scenario $\chi_{SM}^2 = 14.9$, corresponding to a p-value of 0.06. The largest contributions to χ_{SM}^2 come from R_b , A_{FB}^b and σ_{had} and are 5.6, 5.2 and 2.8 respectively. We also perform a χ^2 fit only with δG_R^b and δG_L^b while putting other parameters to zero. In this case $\chi_{min}^2 = 7.8$ with p-value 0.25. The corresponding 1σ and 2σ regions are presented in the left Fig. 4 by red and orange curves, respectively. As expected, the data is mainly sensitive to bottom quark couplings leading to model independent bounds of $\delta G_L^b = 0.002(2)$ and $\delta G_R^b = 0.015(6)$.

Now, we turn to specific models. In the singlet up-type vector-like quark model, tree level modification of δG_L^u and δG_L^c is possible. Taking into account the severe constraint on $\delta X_{uu}^u = -0.0001(6)$ from CKM unitarity, δG_L^u has no significant influence in the fit. Therefore, we use the data to extract the best current constraint on $\delta X_{cc}^u = -0.0020(13)$. The constraint comes essentially from three observables: R_b , σ_{had} and Γ_z , which are more constraining than direct $Z \rightarrow c\bar{c}$ measurements R_c and A_{FB}^c . We calculate the individual contribution to $\Delta\chi^2$ from each observable in the points which are $\pm 1\sigma$ away from the best fit point. Contributions to $\Delta\chi_{-\sigma}^2$ from R_b , σ_{had} , Γ_z , R_c and A_{FB}^c are -1.1 , -0.7 , 2.5 , 0.4 and -0.1 , respectively, while contributions to $\Delta\chi_{+\sigma}^2$ from R_b , σ_{had} , Γ_z , R_c and A_{FB}^c are 1.4 , 1.1 , -1.4 , -0.2 and 0.1 , respectively.

In the singlet down-type vector-like quark model, tree level modifications of δG_L^d , δG_L^s and δG_L^b are possible. APV puts a strong constraint on δX_{dd}^d , so that the Z data can be fitted with only two parameters, δX_{ss}^d and δX_{bb}^d . Results are presented in Fig. 4 right. The best fit point now corresponds to $(\delta X_{bb}^d, \delta X_{ss}^d) = (0.0027, -0.0046)$ where $\chi_{min}^2 = 8.7$. The fit is statistically better than in the SM with a p-value of 0.2. The most relevant observable in the fit is R_b and its contribution to $\chi_{SM}^2 - \chi_{min}^2$ is 5.6, while the contribution of σ_{had} is 1.0. Analyzing one-dimensional χ^2 functions for each observable, we find 1σ preferred regions to be $\delta X_{ss}^d = -0.005(2)$ and $\delta X_{bb}^d = 0.0027(15)$. Finally, including δX_{dd}^d in the fit and taking into account the APV constraint, the preferred region for δX_{ss}^d is reduced to $\delta X_{ss}^d = -0.002(3)$, while the preferred region for δX_{bb}^d is unaffected.

In the doublet vector-like quark model, tree level modification of all right handed couplings of light quarks with Z boson is possible. Therefore, we fit Z-pole observables together with the APV constraint on $Y_{uu}^u - 1.12Y_{dd}^d$ with five parameters Y_{uu}^u , Y_{cc}^u , Y_{dd}^d , Y_{ss}^d and Y_{bb}^d . Marginalizing over four parameters, we get the preferred range for the remaining one. Modification of charm and bottom quark couplings can be constrained to a percent level, $Y_{bb}^d = -0.018(6)$ and $Y_{cc}^u = -0.003(9)$. Negative value for Y_{bb}^d is mainly driven by R_b and A_{FB}^b , which contribute to $\chi_{SM}^2 - \chi_{min}^2$ by 5.5 and 3.5, respectively. In the case of the light quark couplings, observables given in the table can

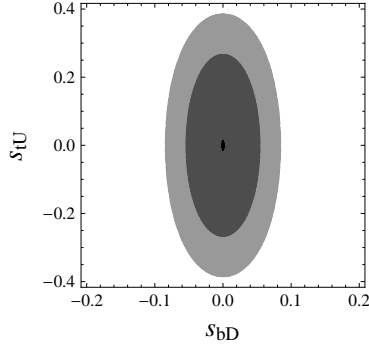


Figure 5: Fit of Z-pole data in the model with a doublet vector-like quark mixing predominantly with the third generation. Best fit point, 1σ (dark gray) and 2σ (light gray) regions are shown in the (s_{bD}, s_{tU}) plane.

not distinguish between different light flavors, giving very poor constraints on one coupling after marginalizing over others. Therefore, we include new observables into the fit which are poorly measured but can distinguish between light quark flavours, namely asymmetries associated with the strange quark, with experimental values $(A^s)_{exp} = 0.895(91)$ and $(A_{FB}^s)_{exp} = 0.0976(114)$ [10]. The constraints we get are rather mild, since the experimental values for A_s and A_{FB}^s have large experimental uncertainties. We obtain the following bounds on $Y_{uu}^u = 0.035(40)$, $Y_{dd}^d = 0.030(35)$ and $Y_{ss}^d = -0.05^{+0.08}_{-0.06}$.

Finally, in the model with one vector-like quark doublet mixing predominantly with the third generation, modification of δG_R^b is induced at tree level $\delta G_R^b = -(1/2)s_{bD}^2$, while modification of δG_L^b is induced at one-loop level

$$\delta G_L^b = \frac{g^2}{64\pi^2} s_{tU}^2 \left(\frac{f_1(x, x')}{r} + f_3(x, x') \right), \quad (C7)$$

where $x \equiv m_t^2/m_W^2$, $x' \equiv m_{u'}^2/m_W^2$ and $r \equiv m_{u'}^2/m_t^2$, and f_1 and f_3 are loop functions given in refs. [34, 65]. The above expression is given in the $x, x' \gg 1$ limit and for small mixing angles. In our numerical evaluation we use the full one-loop expressions and do not assume small mixing angles, even though we note that the above approximations are fairly good. Using the available Z-pole data to fit s_{bD} and s_{tU} parameters, we present the results in the (s_{bD}, s_{tU}) plane in Fig. 5 for fixed $m_{u'} = 800$ GeV. We have checked, however, that the results are mostly insensitive to the precise value of the u' mass in the interesting region ($500 \text{ GeV} < m_{u'} < 1500 \text{ GeV}$). Marginalizing over s_{bD} , we obtain $|s_{tU}| < 0.35$ at 95% C.L..

Appendix D: Doublet vector-like quark contributions to ρ parameter in presence of $1/\Lambda$ corrections

In the renormalizable doublet vector-like quark model, the divergences in the loop calculation of the ρ parameter vanish only after imposing the connection between masses and mixing angles in the up- and down-quark sectors namely

$$M_D = M_U \equiv M_Q, \quad (D1)$$

with

$$\begin{aligned} M_D^2 &= c_{bD}^2 m_{d'}^2 + s_{bD}^2 m_b^2, \\ M_U^2 &= c_{tU}^2 m_{u'}^2 + s_{tU}^2 m_t^2. \end{aligned} \quad (D2)$$

Relation D1 no longer holds after the inclusion of non-renormalizable operators. However, one can still relate the parameters in the up and down sector through the identities (see Sec. V)

$$M_{U,D} \equiv \sqrt{\bar{M}_{U,D}^2 + v^4((c_1^-)^i (c_1^-)_i^*)/4\Lambda^2}, \quad \bar{M}_{U,D} \equiv M_Q \pm v^2 c_2^-/2\Lambda. \quad (D3)$$

Expanding to $\mathcal{O}(1/\Lambda)$, the divergences in ρ again cancel. Building upon known oblique corrections from vector-like quarks in the renormalizable model [66], the new physics contribution to the ρ parameter including leading dimension

5 non-renormalizable operators can then be written as

$$\Delta\rho = \frac{\alpha N_C}{16\pi s_W^2} \left\{ \sum_{i=t,u',j=b,d'} \left[(|\tilde{V}_{ij}^L|^2 + |\tilde{V}_{ij}^R|^2) g_1(x_i, x_j) + 2\text{Re} \left(\tilde{V}_{ij}^L \tilde{V}_{ij}^{R*} \right) g_2(x_i, x_j) \right] - s_{bD}^2 c_{bD}^2 g_1(x_{d'}, x_b) - s_{tU}^2 c_{tU}^2 g_1(x_{u'}, x_t) - g_1(x_t, x_b) + g_{\text{nr}} \right\}, \quad (\text{D4})$$

where $x_i \equiv m_i^2/m_W^2$. The corresponding mixing matrices are defined as $(\tilde{V}^L)_{ij} \equiv (\tilde{U}_u^L)_{ik} (\tilde{U}_d^L)_{jk}^*$ and $(\tilde{V}^R)_{ij} \equiv (\tilde{U}_u^R)_{ik} (\tilde{U}_d^R)_{jk}^*$, where

$$\tilde{U}_{u,d}^R = \begin{pmatrix} c_{tU,bD} & s_{tU,bD} \\ -s_{tU,bD} & c_{tU,bD} \end{pmatrix}, \quad \tilde{U}_{u,d}^L = \begin{pmatrix} c'_{tU,bD} & s'_{tU,bD} \\ -s'_{tU,bD} & c'_{tU,bD} \end{pmatrix}. \quad (\text{D5})$$

The relevant loop functions are given by

$$g_1(x_1, x_2) \equiv x_1 + x_2 - \frac{2x_1x_2}{x_1 - x_2} \ln \frac{x_1}{x_2}, \quad (\text{D6})$$

$$g_2(x_1, x_2) \equiv 2\sqrt{x_1x_2} \left(\frac{x_1 + x_2}{x_1 - x_2} \ln \frac{x_1}{x_2} - 2 \right), \quad (\text{D7})$$

while the new term which incorporates explicit effects due to $\mathcal{O}(1/\Lambda)$ non-renormalizable mass-splitting operators reads

$$g_{\text{nr}} = 4\delta \left\{ s_{bD}^2 x_b \ln \frac{x_b}{x_{d'}} - s_{tU}^2 x_t \ln \frac{x_t}{x_{u'}} + x_U \ln \frac{x_{d'}}{x_{u'}} \right\}, \quad (\text{D8})$$

with $\delta \equiv (M_U - M_D)/M_U$ and $M_{U,D}$ given in [D2](#) (note that x_U refers to M_U^2/m_W^2).

-
- [1] G. Aad *et al.* [ATLAS Collaboration], Phys. Lett. B **716** (2012) 1 [[arXiv:1207.7214](#) [hep-ex]]; S. Chatrchyan *et al.* [CMS Collaboration], Phys. Lett. B **716** (2012) 30 [[arXiv:1207.7235](#) [hep-ex]].
- [2] M. Papucci, J. T. Ruderman and A. Weiler, JHEP **1209**, 035 (2012) [[arXiv:1110.6926](#) [hep-ph]].
- [3] N. Arkani-Hamed, A. G. Cohen and H. Georgi, Phys. Lett. B **513**, 232 (2001) [[hep-ph/0105239](#)]; N. Arkani-Hamed, A. G. Cohen, T. Gregoire and J. G. Wacker, JHEP **0208**, 020 (2002) [[hep-ph/0202089](#)]; N. Arkani-Hamed, A. G. Cohen, E. Katz, A. E. Nelson, T. Gregoire and J. G. Wacker, JHEP **0208**, 021 (2002) [[hep-ph/0206020](#)]; M. Perelstein, M. E. Peskin and A. Pierce, Phys. Rev. D **69**, 075002 (2004) [[hep-ph/0310039](#)]; T. Han, H. E. Logan, B. McElrath and L. -T. Wang, Phys. Rev. D **67**, 095004 (2003) [[hep-ph/0301040](#)].
- [4] R. Contino, L. Da Rold and A. Pomarol, Phys. Rev. D **75**, 055014 (2007) [[hep-ph/0612048](#)]; C. Anastasiou, E. Furlan and J. Santiago, Phys. Rev. D **79**, 075003 (2009) [[arXiv:0901.2117](#) [hep-ph]]; O. Matsedonskyi, G. Panico and A. Wulzer, JHEP **1301**, 164 (2013) [[arXiv:1204.6333](#) [hep-ph]]; G. Panico, M. Redi, A. Tesi and A. Wulzer, JHEP **1303**, 051 (2013) [[arXiv:1210.7114](#) [hep-ph]]; M. Redi and A. Tesi, JHEP **1210**, 166 (2012) [[arXiv:1205.0232](#) [hep-ph]]; L. Vecchi, [arXiv:1304.4579](#) [hep-ph].
- [5] G. F. Giudice, C. Grojean, A. Pomarol and R. Rattazzi, JHEP **0706**, 045 (2007) [[hep-ph/0703164](#)].
- [6] R. Contino, M. Ghezzi, C. Grojean, M. Muhlleitner and M. Spira, [arXiv:1303.3876](#) [hep-ph].
- [7] A. Azatov and J. Galloway, Phys. Rev. D **85**, 055013 (2012) [[arXiv:1110.5646](#) [hep-ph]]; J. Berger, J. Hubisz and M. Perelstein, JHEP **1207**, 016 (2012) [[arXiv:1205.0013](#) [hep-ph]]; A. Carmona and F. Goertz, [arXiv:1301.5856](#) [hep-ph].
- [8] J. A. Aguilar-Saavedra, Phys. Rev. D **67**, 035003 (2003) [Erratum-ibid. D **69**, 099901 (2004)] [[hep-ph/0210112](#)].
- [9] R. J. Dowdall, C. T. H. Davies, G. P. Lepage and C. McNeile, [arXiv:1303.1670](#) [hep-lat].
- [10] J. Beringer *et al.* [Particle Data Group Collaboration], Phys. Rev. D **86**, 010001 (2012).
- [11] A. J. Buras, K. Gemmler and G. Isidori, Nucl. Phys. B **843**, 107 (2011) [[arXiv:1007.1993](#) [hep-ph]].
- [12] E. Golowich, J. Hewett, S. Pakvasa and A. A. Petrov, Phys. Rev. D **76**, 095009 (2007) [[arXiv:0705.3650](#) [hep-ph]].
- [13] Y. Amhis *et al.* [Heavy Flavor Averaging Group Collaboration], [arXiv:1207.1158](#) [hep-ex].
- [14] B. Grzadkowski and M. Misiak, Phys. Rev. D **78**, 077501 (2008) [Erratum-ibid. D **84**, 059903 (2011)] [[arXiv:0802.1413](#) [hep-ph]]; J. Drobnak, S. Fajfer and J. F. Kamenik, Phys. Lett. B **701**, 234 (2011) [[arXiv:1102.4347](#) [hep-ph]]; J. F. Kamenik, M. Papucci and A. Weiler, Phys. Rev. D **85**, 071501 (2012) [[arXiv:1107.3143](#) [hep-ph]]; J. Drobnak, S. Fajfer and J. F. Kamenik, Nucl. Phys. B **855**, 82 (2012) [[arXiv:1109.2357](#) [hep-ph]]; C. Zhang, N. Greiner and S. Willenbrock, Phys. Rev. D **86**, 014024 (2012) [[arXiv:1201.6670](#) [hep-ph]].

- [15] T. P. Cheng and M. Sher, Phys. Rev. D **35**, 3484 (1987).
- [16] G. Blankenburg, J. Ellis and G. Isidori, Phys. Lett. B **712**, 386 (2012) [[arXiv:1202.5704](#) [hep-ph]]; R. Harnik, J. Kopp and J. Zupan, JHEP **1303**, 026 (2013) [[arXiv:1209.1397](#) [hep-ph]].
- [17] [ATLAS Collaboration], Note ATLAS-CONF-2013-034 [<http://cds.cern.ch/record/1528170>].
- [18] CMS-PAS-HIG-12-045
- [19] A. D. Martin, W. J. Stirling, R. S. Thorne and G. Watt, Eur. Phys. J. C **63**, 189 (2009) [[arXiv:0901.0002](#) [hep-ph]].
- [20] R. D. Ball, M. Bonvini, S. Forte, S. Marzani and G. Ridolfi, [arXiv:1303.3590](#) [hep-ph].
- [21] C. a. D. C. a. t. T. N. P. a. H. W. Group [Tevatron New Physics Higgs Working Group and CDF and D0 Collaborations], [arXiv:1207.0449](#) [hep-ex].
- [22] A. Djouadi, W. Kilian, M. Muhlleitner and P. M. Zerwas, Eur. Phys. J. C **10**, 45 (1999) [[hep-ph/9904287](#)].
- [23] A. Djouadi, “The Anatomy of electro-weak symmetry breaking. I: The Higgs boson in the standard model,” Phys. Rept. **457**, 1 (2008) [[hep-ph/0503172](#)].
- [24] G. Cacciapaglia, A. Deandrea, G. D. La Rochelle and J. -B. Flament, JHEP **1303**, 029 (2013) [[arXiv:1210.8120](#) [hep-ph]]; G. Belanger, B. Dumont, U. Ellwanger, J. F. Gunion and S. Kraml, JHEP **1302**, 053 (2013) [[arXiv:1212.5244](#) [hep-ph]].
- [25] [ATLAS Collaboration], Note ATLAS-CONF-2013-013, [<http://cds.cern.ch/record/1523699>].
- [26] [ATLAS Collaboration], Note ATLAS-CONF-2013-030, [<http://cds.cern.ch/record/1527126>].
- [27] [ATLAS Collaboration], Note ATLAS-CONF-2013-012, [<http://cds.cern.ch/record/1523698>].
- [28] [CMS Collaboration], Note CMS-PAS-HIG-13-003, [<http://cds.cern.ch/record/1523673>].
- [29] [CMS Collaboration], Note CMS-PAS-HIG-13-002, [<http://cds.cern.ch/record/1523767>].
- [30] Talk by Christophe Ochoa, Moriond QCD and High Energy Interactions, 14.03.2013.
- [31] [CMS Collaboration], Note CMS-PAS-HIG-13-004, [<http://cds.cern.ch/record/1528271>]; Talk by Mingshui Chen, Rencontres de Moriond EW, 06.03.2013; Talk by Valentina Duta, Rencontres de Moriond EW, 06.03.2013.
- [32] C. Delaunay, C. Grojean and G. Perez, [arXiv:1303.5701](#) [hep-ph].
- [33] J. Kearney, A. Pierce and N. Weiner, Phys. Rev. D **86**, 113005 (2012) [[arXiv:1207.7062](#) [hep-ph]]; G. Moreau, Phys. Rev. D **87**, 015027 (2013) [[arXiv:1210.3977](#) [hep-ph]].
- [34] S. Dawson and E. Furlan. A Higgs Conundrum with Vector Fermions. Phys.Rev., D86:015021, 2012, [arXiv:1205.4733](#).
- [35] [ATLAS Collaboration], Note ATLAS-CONF-2013-018, [<http://cds.cern.ch/record/1525525>].
- [36] D. Carmi, A. Falkowski, E. Kuflik and T. Volansky, JHEP **1207** (2012) 136 [[arXiv:1202.3144](#) [hep-ph]].
- [37] F. Garberon and T. Golling, [arXiv:1301.4454](#) [hep-ex].
- [38] G. Aad *et al.* [ATLAS Collaboration], Phys. Rev. D **86**, 012007 (2012) [[arXiv:1202.3389](#) [hep-ex]].
- [39] N. Bonne and G. Moreau, Phys. Lett. B **717**, 409 (2012) [[arXiv:1206.3360](#) [hep-ph]].
- [40] A. Azatov, O. Bondu, A. Falkowski, M. Felcini, S. Gascon-Shotkin, D. K. Ghosh, G. Moreau and S. Sekmen, Phys. Rev. D **85**, 115022 (2012) [[arXiv:1204.0455](#) [hep-ph]].
- [41] [CMS Collaboration], Note CMS-PAS-TOP-12-035, [<http://cds.cern.ch/record/1520879>].
- [42] N. Kidonakis, Phys. Rev. D **83**, 091503 (2011) [[arXiv:1103.2792](#) [hep-ph]].
- [43] G. Aad *et al.* [ATLAS Collaboration], Phys. Lett. B **717**, 330 (2012) [[arXiv:1205.3130](#) [hep-ex]].
- [44] S. Chatrchyan *et al.* [CMS Collaboration], JHEP **1212**, 035 (2012) [[arXiv:1209.4533](#) [hep-ex]].
- [45] G. Aad *et al.* [ATLAS Collaboration], JHEP **1209**, 139 (2012) [[arXiv:1206.0257](#) [hep-ex]].
- [46] J. A. Aguilar-Saavedra, Nucl. Phys. B **804**, 160 (2008) [[arXiv:0803.3810](#) [hep-ph]].
- [47] M. Fischer, S. Groote, J. G. Korner and M. C. Mauser, Phys. Rev. D **63**, 031501 (2001) [[hep-ph/0011075](#)].
- [48] J. Drobnak, S. Fajfer and J. F. Kamenik, Phys. Rev. D **82**, 114008 (2010) [[arXiv:1010.2402](#) [hep-ph]].
- [49] G. Aad *et al.* [ATLAS Collaboration], JHEP **1206**, 088 (2012) [[arXiv:1205.2484](#) [hep-ex]].
- [50] G. D’Ambrosio, G. Isidori and J. Portoles, Phys. Lett. B **423**, 385 (1998) [[hep-ph/9708326](#)]; G. Isidori and R. Unterdorfer, JHEP **0401**, 009 (2004) [[hep-ph/0311084](#)].
- [51] T. Inami and C. S. Lim, Prog. Theor. Phys. **65**, 297 (1981) [Erratum-ibid. **65**, 1772 (1981)].
- [52] A. J. Buras, J. Girrbach, D. Guadagnoli and G. Isidori, Eur. Phys. J. C **72**, 2172 (2012) [[arXiv:1208.0934](#) [hep-ph]].
- [53] J. Laiho, E. Lunghi and R. S. Van de Water, Phys. Rev. D **81**, 034503 (2010) [[arXiv:0910.2928](#) [hep-ph]]. Updates available on <http://latticeaverages.org/>.
- [54] C. M. Bouchard, E. D. Freeland, C. Bernard, A. X. El-Khadra, E. Gamiz, A. S. Kronfeld, J. Laiho and R. S. Van de Water, PoS LATTICE **2011**, 274 (2011) [[arXiv:1112.5642](#) [hep-lat]].
- [55] A. Lenz, U. Nierste, J. Charles, S. Descotes-Genon, A. Jantsch, C. Kaufhold, H. Lacker and S. Monteil *et al.*, Phys. Rev. D **83**, 036004 (2011) [[arXiv:1008.1593](#) [hep-ph]].
- [56] A. Crivellin and L. Mercolli, Phys. Rev. D **84**, 114005 (2011) [[arXiv:1106.5499](#) [hep-ph]].
- [57] P. del Amo Sanchez *et al.* [BABAR Collaboration], Phys. Rev. D **82**, 051101 (2010) [[arXiv:1005.4087](#) [hep-ex]]; W. Wang, [arXiv:1102.1925](#) [hep-ex].
- [58] RAaij *et al.* [LHCb Collaboration], Phys. Rev. Lett. **110**, 021801 (2013) [[arXiv:1211.2674](#) [Unknown]].
- [59] G. C. Branco, L. Lavoura and J. P. Silva, Int. Ser. Monogr. Phys. **103**, 1 (1999).
- [60] U. Haisch and S. Westhoff, JHEP **1108**, 088 (2011) [[arXiv:1106.0529](#) [hep-ph]].
- [61] M. I. Gresham, I. -W. Kim, S. Tulin and K. M. Zurek, Phys. Rev. D **86**, 034029 (2012) [[arXiv:1203.1320](#) [hep-ph]].
- [62] V. A. Dzuba, J. C. Berengut, V. V. Flambaum and B. Roberts, [arXiv:1207.5864](#) [hep-ph].
- [63] S. Schael *et al.* [ALEPH and DELPHI and L3 and OPAL and SLD and LEP Electroweak Working Group and SLD Electroweak Group and SLD Heavy Flavour Group Collaborations], Phys. Rept. **427**, 257 (2006) [[hep-ex/0509008](#)].
- [64] M. Baak, M. Goebel, J. Haller, A. Hoecker, D. Kennedy, R. Kogler, K. Moenig and M. Schott *et al.*, Eur. Phys. J. C **72** (2012) 2205 [[arXiv:1209.2716](#) [hep-ph]].

- [65] P. Bamert, C.P. Burgess, James M. Cline, David London, and E. Nardi. R(b) and new physics: A Comprehensive analysis. Phys.Rev., D54:42754300, 1996.
- [66] L. Lavoura and J. P. Silva, Phys. Rev. D **47**, 2046 (1993).